Spatio-temporal co-variability of air pollutants and meteorological variables over Haqel and Jeddah, Saudi Arabia

Syeda Batool TAZEEM[1], Ahmed NABEEL[2] and Hussain ATHAR[1,3]*

[1]Department of Meteorology, COMSATS University, Islamabad 45550, Pakistan.
[2]School of Engineering & Applied Sciences (SEAS), ISRA University, Islamabad 44000, Pakistan.
[3]Centre for Climate Research and Development, COMSATS University, Islamabad 45550, Pakistan.
*Corresponding author; email: athar.hussain@comsats.edu.pk

RESUMEN

Este estudio presenta una primera evaluación simultánea de la tendencia y la magnitud de los contaminantes atmosféricos (CO, H_2S, SO_2, NO_2, NO, NO_X, O_3 y PM_{10}) y las variables meteorológicas (precipitación [RF], humedad relativa [RH], presión atmosférica [PR], temperatura [TC], velocidad del viento [WS] y dirección del viento [WD]) en la ciudad de Haqel y en cuatro lugares diferentes de la ciudad de Jeddah, Arabia Saudí, durante un periodo continuo de cinco años (2008-2012). Se describen las covariaciones espacio-temporales de los contaminantes atmosféricos en cuanto a sus ciclos diurnos, semanales, estacionales y anuales, y su relación con las condiciones meteorológicas, junto con las estimaciones del efecto de fin de semana. Se observó una tendencia anual decreciente para la mayoría de los contaminantes atmosféricos analizados, excepto para el O_3 y las PM_{10}. El CO, NO_2, NO y NO_x mostraron un fuerte efecto de fin de semana. Un análisis de cambio basado en percentiles mostró un aumento de las concentraciones de O_3 (PM_{10}) en los percentiles inferiores (superiores) de la primera a la segunda mitad del periodo de estudio. El estudio identificó 12 fenómenos meteorológicos ciclónicos durante el periodo de cinco años asociados a altas concentraciones de PM_{10} (> 500 µg m^{-3}) en relación con un valor medio de 102 µg m^{-3}, con una desviación estándar de 179 µg m^{-3}. El estudio también analizó los impactos de varios eventos anticiclónicos de latitudes medias en las concentraciones de contaminantes atmosféricos y encontró un cambio significativo en las concentraciones de contaminantes atmosféricos (CO, SO_2, NO_2, NO, NO_x, O_3 y PM_{10}) y en las variables meteorológicas (HR, PR, TC, WS y WD) asociadas con las condiciones de aire superior estancado durante el bloqueo atmosférico.

ABSTRACT

This study presents a first simultaneous trend and magnitude assessment of air pollutants (CO, H_2S, SO_2, NO_2, NO, NO_x, O_3 and PM_{10}) and meteorological variables (rainfall [RF], relative humidity [RH], atmospheric pressure [PR], temperature [TC], wind speed [WS], and wind direction [WD]) in the city of Haqel and at four different locations in the city of Jeddah, Saudi Arabia, for a continuous 5-year period (2008-2012). The spatio-temporal co-variations of air pollutants in terms of their diurnal, weekly, seasonal and annual cycles, and their relationship with meteorological conditions, along with the estimates of the weekend effect, are described. A decreasing annual trend was observed for most air pollutants analyzed except for O_3 and PM_{10}. The CO, NO_2, NO and NO_x displayed a strong weekend effect. A percentile-based change analysis displayed an increase in concentrations for O_3 (PM_{10}) in the lower (higher) percentiles from the first to second half of the study period. The study identified 12 cyclonic weather events during the 5-year time period associated with high PM_{10} concentrations (> 500 µg m^{-3}) relative to a mean value of 102 µg m^{-3}, with a standard deviation value of 179 µg m^{-3}. The study also analyzed the impacts of several mid-latitude anti-cyclonic events on air pollutant concentrations and found a significant change in air pollutant concentrations (CO, SO_2, NO_2, NO, NO_x, O_3 and PM_{10}) and meteorological variables (RH, PR, TC, WS, and WD) associated with stagnant upper air conditions during the atmospheric blocking.

Keywords: air pollutant characterization, weekend effect, extreme events, blocking impacts, Saudi Arabia.

1. Introduction

Air pollutants (gases and particles) are a matter of great interest due to their impacts on climate and public health (IPCC, 2014, 2021; Abbass et al., 2017; Soleimani et al., 2020). Although air pollutants are a very small fraction of the Earth's atmospheric composition, they contribute to climate forcing and affect the hydrological cycle (Hinds, 1999; Ramanathan et al., 2001). Air pollutants play a critical role in the reproduction of biological organisms and in causing or enhancing diseases (Pöschl, 2005; Amsalu et al., 2019; Li et al., 2019; Peeples, 2020; Romano et al., 2020). Air pollutants originate from a variety of natural and man-made sources (Hidy, 2019). Particles may be divided into two categories: primary particles that are emitted directly into the atmosphere in liquid or solid form from burning of biomass and fossil fuel, volcanic eruptions, wind-forced suspension of mineral dust, sea salt and biological materials (Tomasi et al., 2017); and secondary particles that form by nucleation, condensation and reaction of gaseous precursors. Both primary and secondary particles are distributed in the atmosphere through turbulent mixing and wind transport (NASEM, 2016). Air pollutants, with a short life span of about a week in the troposphere, generally disperse from the source of origin and are highly variable spatio-temporally (Kedia and Ramachandran, 2009). In the troposphere, the diameter and mass concentration of air borne particles typically vary in range between 10^{-9}-10^{-4} m and 1-100 µg m^{-3}, respectively (Hinds, 1999; Raes et al., 2000; Pöschl, 2005).

To better understand the role of air pollutants in the tropospheric chemistry, a detailed characterization of air pollutants from in-situ and remotely sensed observations is needed (Kaufman et al., 1997). The air pollutants focused in this study include carbon monoxide (CO), sulphur dioxide (SO_2), hydrogen sulfide (H_2S), nitrogen oxides (NO_2, NO, NO_x), ozone (O_3), and particulate matter (PM_{10}). CO, SO_2 and NO_2 are hazardous gases produced by, for instance, fuel burning. H_2S is also a toxic gas emitted into the atmosphere by organic material decomposition and fuel refining. Surface O_3 has detrimental effects on public health, agriculture and the associated ecosystems; it is not directly released into the atmosphere, but is formed as a product of interaction between NO_x and volatile organic compounds (VOCs) in the presence

of sunlight. PM_{10} particles, having an aerodynamic diameter less than or equal to 10 µm, can be found in different shapes varying from irregular, platy, spherical, rod-like to angular. It is of great concern due to its adverse effects on humans and environment (Raizenne et al., 1996; Tawabini et al., 2017).

Investigation of spatio-temporal distributions of air pollutants, their cross-effect and the influence of meteorological variables such as atmospheric pressure, temperature, rainfall, relative humidity, wind speed and direction (PR, TC, RF, RH, WS, and WD, respectively) on air pollutant properties is essential for an understanding of climatology and spatio-temporal distribution characteristics of air pollutants (NASEM, 2016; Ordóñez et al., 2019; Rahman et al., 2019). Meteorological variables influence air quality not only on short term basis (daily and weekly) but also on long term basis, i.e., seasonally and annually (Zhang et al., 2018a).

Given that considerable challenges on the availability of air quality data remain in developing countries (Alvarado et al., 2019; Brauer et al., 2019; Pinder et al., 2019), it is not surprising that only a few studies have been carried out for the characterization of air pollutants in the region of Saudi Arabia: Hassan et al. (2013) monitored NO, NO_2 and O_3 in Jeddah city; Al-Jeelani (2014) investigated the diurnal and seasonal variations of surface O_3 and its precursors, and SO_2 in the atmosphere of Yanbu; Alghamdi et al. (2014) analyzed diurnal and seasonal variations of O_3 and NO_x concentrations in Jeddah city; Lihavainen et al. (2016, 2017) analyzed air pollutant concentrations in Hada Al Sham in western Saudi Arabia using single ground monitoring station data.

Dust events occur all year round in Saudi Arabia, with maximum intensity during spring and summer (Mayer, 1999; Yu et al., 2013; Maghrabi and Al-Dosari, 2016; Namdari et al., 2018). Dust storms are found to elevate PM_{10} concentration (Al-Hemoud et al., 2018). Relatively little attention has been given to cyclonic and anti-cyclonic extreme weather events in previous studies in relation to air pollutants. Weather events that encompass large spatio-temporal fluctuations in air pollutants play an important role in socio-economic life. As the study area is highly prone to dust events, this study also considers in some detail the detection of changes in air pollutant concentrations associated with extreme weather events (Tazeem, 2018).

Thus, this study focuses on understanding the spatio-temporal characteristics of extreme air pollutant events and its interdependency on meteorological variables. An added value of this study is to assess the relationship between air pollutants and meteorological variables using in-situ observations for an extended continuous period of 5 years (2008-2012); such a detailed study has not been previously done in the data-sparse region of Saudi Arabia.

2. Data and methodology

2.1 Data

2.1.1 Study area and ground-based data

Saudi Arabia is located in Southwest Asia and covers almost 80% of the Arabian Peninsula area (Vincent, 2008). It lies between 16-32º N latitude and 34-56º E longitude, and has one of the warmest and most arid climates of the world (Athar, 2014). There are no large inland water bodies except for the Red Sea bordering the west, whereas the Arabian Gulf borders east of Saudi Arabia, and Oman and Yemen to the south. Haqel is a relatively small city near the Red Sea, approximately 5 km away from the Jordanian border in northwest Saudi Arabia (Fig. 1). The region of Jeddah comprises three different geomorphological zones; the Red Sea and shoreline, the coastal plain, and low-lying coastal hills and pediments in the east.

The data collected from five different ground-based stations for air pollutants includes CO, H_2S, SO_2, NO_2, NO, NO_x, O_3 and PM_{10} and meteorological variables include RF, RH, PR, TC, WS and WD from January 2008 to October 2012, with an observation frequency of 15 min. Data was obtained from the Presidency of Meteorology and Environment, Jeddah, for five air quality monitoring stations, with four located in Jeddah: Abhur (ABR), Stadium (STA), Bani Malik (BNI) and Industrial area (IDL), and one located in Haqel (HQL). Table I displays the latitude/ longitude, elevation and data availability period of the five air quality monitoring stations from which data was obtained.

The ABR station is located at the sea bay near the east coast of the Red Sea, 30 km from Jeddah city. It is a tourist destination surrounded by a number of resorts, and thus contributes to both fixed and mobile sources of anthropogenic emissions. The STA station is located in the middle of the residential area of Jeddah city, and thus contributes dominantly to fixed sources of anthropogenic emissions. The BNI station is located in a busy shopping area, in the sub-urban corner of the main city, and thus contributes to both types of anthropogenic emissions. The IDL station is located near Jeddah's industrial city, and thus is a source of industrial pollutants (such as SO_2). The HQL station is located in sub-urban area of Haqel city, and thus has less vehicular related emissions. It is a source of more anthropogenic surface O_3 emissions.

2.1.2 Satellite and reanalysis-based data

In this study, remotely sensed aerosol optical depth (AOD) observations were utilized. They were obtained from the ozone monitoring instrument (OMI) at 442 nm. The remotely sensed data is also utilized to study the behavior of meteorological variables, including atmospheric infrared sounder-based geopotential height at 925 hPa (AIRS H_{925}). For some recent reviews and applications that use satellite data for assessing regional air quality see, e.g., Engel-Cox et al. (2004), Martin (2008), Kumar et al. (2018), Sowden et al. (2018), Ali et al. (2020), Stirnberg et al. (2020).

Furthermore, the 10 m average daily wind data was obtained from the National Centers for Environmental Prediction/National Center for Atmospheric Research (NCEP/NCAR), Boulder, CO, USA. This global gridded wind data is available at a horizontal resolution of 2.5º × 2.5º, separately for the u and v wind components (Kalnay et al., 1996).

2.2 Methodology

2.2.1 Quality control

Multiple quality control measures were performed on the data prior to analysis throughout the study period (Athar, 2014). Values greater than 3σ were checked for extreme events from a 5-year average. Monthly and yearly averages were computed with at least 70% availability of the data (Mora et al., 2017). The minimum (maximum) number of missing days for STA (HQL) were 9.28% (26.23%). The data was stratified at different time scales and whenever possible compared with the USA based Environmental Protection Agency (EPA) air quality standards.

An air quality index (AQI) is devised to help understand the air quality of an area. According to the USEPA, an AQI index of more than 100 indicates
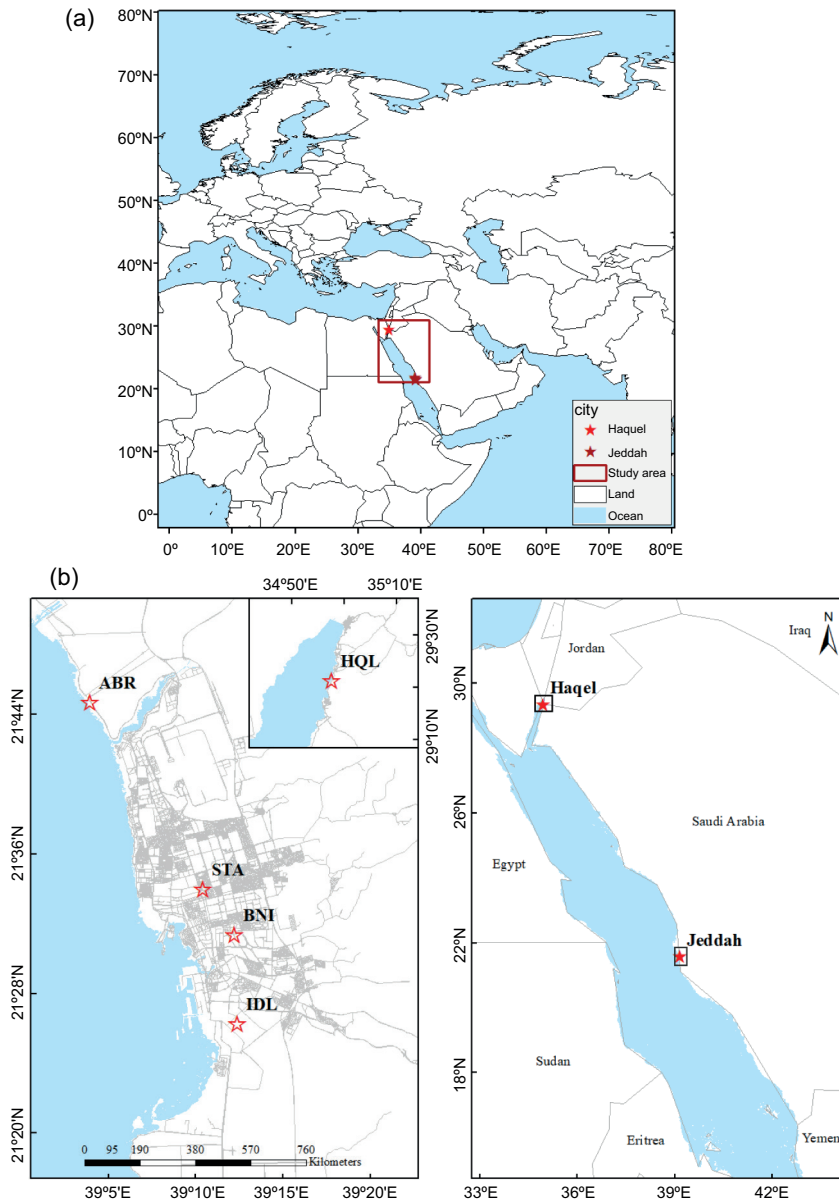
Fig. 1. (a) Map of the study area indicating location of the monitored sites and an averaging box encompassing all monitoring stations. (b) Location of the five monitoring stations for air pollutants and meteorological variables in Haqel and Jeddah, Saudi Arabia.

Table I. Details of air quality and meteorological variables monitoring stations, including latitude/longitude, elevation and start and end date of data availability.

Station	Abbreviation	Latitude (N)	Longitude (E)	Elevation (m)	Start date	End date
Haqel	HQL	29°21′18.62″	34°57′39.98″	12.19	01/01/08	13/10/12
Abhur	ABR	21°44′40.45″	39°03′56.06″	6.70	01/03/08	13/10/12
Stadium	STA	21°33′57.87″	39°10′24.51″	18.59	01/01/08	13/10/12
Bani Malik	BNI	21°31′22.95″	39°12′11.14″	18.28	01/01/09	13/10/12
Industrial	IDL	21°26′16.27″	39°12′22.60″	13.11	01/06/08	13/10/12

(a moderately) unhealthy air quality and correspond to a certain level of air pollutants, i.e., 10.35 mg m^{-3} of CO and 147 µg m^{-3} of O_3 averaged over 8 h, 196.5 µg m^{-3} of SO_2 averaged over 1 h, and 150 µg m^{-3} PM_{10} averaged over 24 h.

The percentiles computed for air pollutants were compared with the EPA based AQI values for CO, SO_2, O_3 and PM_{10} for the following three classes: low (0-50), moderate (51-150), and high (151-300). A comparison of the percentiles for four air pollutants (O_3, CO, SO_2 and PM_{10}) with the AQI is presented via box whisker plots in Figure 2.

2.2.2 Temporal variations

The data was temporally stratified on an hourly, daytime, nighttime, weekly, monthly, seasonal and annual basis. The seasonal variations were analyzed using March-May as spring of June-August as summer, November-October as autumn, and December-February as winter, whereas November-April are considered as the wet season and June-September as the dry season (Athar, 2015).

Computation of the weekend effect was also carried out to identify anthropogenic origins. In Saudi Arabia, weekdays are from Saturday to Thursday, with Friday as weekend. The weekend effect is thus considered as the difference between the weekend (Friday) and weekdays (Saturday-Thursday) values.

2.2.3 Percentile-based analysis

Percentiles are considered as an effective statistical measure for the analysis of trends because of their independency on skewness of data and on extreme values or outliers (Wilks, 2020). Percentile-based analysis is used to assess variation in low to high concentration scales (Iqbal and Athar, 2018). Data was divided into two half intervals to study percentile variability. Percentiles for each interval and the difference between the two halves was analyzed.

2.2.4 Extreme events

Modulations in air pollutant concentrations associated with cyclonic extreme events were noticed earlier in Riyadh, Saudi Arabia (Alharbi et al., 2013), as well as on larger scales, encompassing much of the Arabian Peninsula (Prakash et al., 2015). Climatologically, dust storm events occur dominantly in spring and summer in the Arabian Peninsula (Albaqami, 2019).
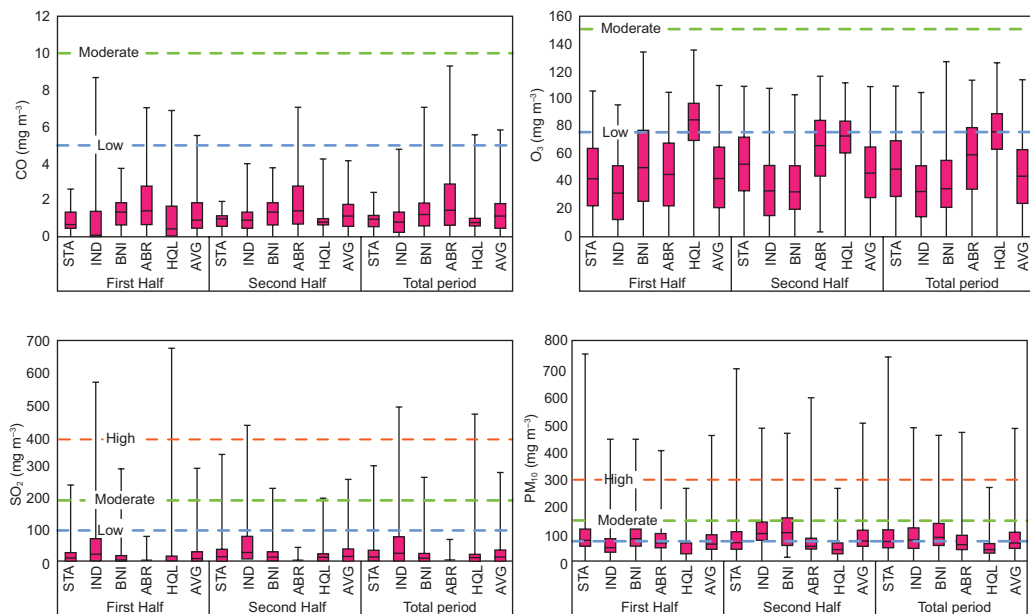
Fig. 2. Box whisker plots of 8-h averages of CO and O_3 (upper row panels); 1-h averages of SO_2 and 24-h averages of PM_{10} (lower row panels), at each station and their average, during the first and second halves, and the total time, of the study period (2008-2012). The horizontal dashed lines in each panel indicate USA-EPA air quality index levels.

Such extreme weather events were identified in the data and were compared with AOD measurements for validation over the study area.

The behavior of meteorological variables was also observed using AIRS H_{925} data. Wind data, obtained from the NCEP/NCAR reanalysis, was then used as visual aid to validate the presence of extreme weather events. The study aims to supplement trends tentatively presented in previous studies and to assess the relationship between air pollutants and meteorological extreme events.

2.2.5 Blocking events

Atmospheric anti-cyclonic blocking events occur when a high-pressure weather system persists for a number of days or weeks (for a recent discussion, see Woollings et al., 2018; Luo and Zhang, 2020). This persistence can lead to extreme weather conditions such as heat waves or cold spells and severe air pollution episodes due to air stagnation. In this study, blocking events recorded by the Global Climate Change Group of the University of Missouri (Colorado, USA) were analyzed and compared with ground and satellite-based observations to assess characteristics of blocking events and their association with high PM_{10}, O_3 and other air pollutant levels in the study region during the 5-year study period (2008-2012).

Blocking events with high PR centers at 30º to 50º E were analyzed in the study (Fig. 1). To diagnose the implications of these phenomena in the study area, blocking events from the catalog were checked for significant deviations from non-blocking periods using the Student t test for air pollutant concentrations and meteorological variables. Average measurements of AOD, O_3, NO_2, SO_2 and CO vertical column for the study area during the blocking period were compared with blocking lifetime periods and with the length of non-blocking periods before and after blocking (nine days for short-span blocking event and 17 days for long-span blocking events) to assess the differences in daily means. Ground-based daily data of air pollutants and meteorological variables for all stations were also averaged and compared to identify statistical differences before, during and after the blocking period, if any (Table II).

True color composite satellite images of the selected blocking and dust storm events depicting the spatial extent of the dust are presented in Figure 3. These images proceed from the Moderate Resolution Imaging Spectroradiometer (MODIS) of the National Aeronautics and Space Administration (NASA), and were downloaded from NASA's worldview website. The black strip in images depicts the swath error (missing data) between two consecutive swath paths. The white area in MODIS images depicts clouds, whereas the light brown color represents dust storms. The spatial and temporal resolution of MODIS images is 500 m and 3-7 days. The time of image acquisition is approximately 10:30 LT.

Commonly used statistical measures such as mean, standard deviation and linear regression fits based on ordinary least square method, are employed to assess the relative changes in air pollutants and meteorological variables during the study period (Wilks, 2020).

3. Results and discussion

3.1 Diurnal, monthly and seasonal variations

On the diurnal time scales, NO_2, NO and NO_x concentrations were higher during the traffic rush hours (7:00 to 9:00 LT) and in the evening. Low concentrations were observed during midday caused by high TC and an increase in photochemical production of O_3 (Fig. 4 and Fig. S1 in the supplementary material). Alghamdi et al. (2014) observed a similar diurnal cycle of NO and NO_2 with peak concentrations at 6:00 to 8:00 LT in spring, autumn and winter, and 24:00-2:00 LT and 5:00-6:00 LT during summer with a decreased concentration in late afternoon and then an increase in nighttime. The highest O_3 concentrations were observed during the afternoon when faster winds blow due to an increase in TC. Analysis of extreme values of O_3 indicated that high values are related to high WS during day time.

Lowest O_3 concentrations were recorded at 7:00 LT, i.e., during the rush hour and with increased emission of NO_x. The diurnal variation of CO was similar to NO_x with peak concentrations during rush hours, while SO_2 exhibited a single concentration peak during during afternoon hours (12:00 to 18:00 LT). A similar SO_2 behavior was noticed during winter months in Bhubaneswar, India during 2010-2012 (Mallik et al., 2019). Only IDL exhibited peak concentrations in H_2S in afternoon hours. A temporal

Table II. Dates of blocking events and their central longitude, including details of satellite based and in situ observations of air pollutants and meteorological variables. Statistically significant differences between before-during, during-after and before-after the blocking period are marked with vertical arrows next to the corresponding variables.

Blocking dates	Longitude (ºE)	Satellite variables		In situ variables	
		Air pollutant	Meteorological variables	Air pollutant	Meteorological variables
03/06/08-09/06/08	50	-	-	-	TC ($\downarrow\uparrow\downarrow$) WS ($\uparrow\downarrow\uparrow$)
11/06/08-19/06/08	50	AOD ($\downarrow\uparrow\downarrow$) O_3 ($\uparrow\downarrow\uparrow$)	-	-	WS ($\uparrow\downarrow\downarrow$)
15/07/08-24/07/08	40	O_3 ($\uparrow\downarrow\uparrow$)	H_{500} ($\downarrow\uparrow\downarrow$)	CO ($\uparrow\downarrow\uparrow$)	-
02/05/09-24/05/09	40	AOD ($\downarrow\uparrow\downarrow$)	H_{500} ($\downarrow\uparrow\uparrow$)	NO_2, NO, NO_X, ($\downarrow\uparrow\downarrow$) CO, O_3 ($\downarrow\uparrow\uparrow$)	PR, WS ($\uparrow\downarrow\downarrow$)
02/09/09-08/09/09	50	O_3 ($\downarrow\uparrow\uparrow$)	-	NO_X ($\downarrow\uparrow\uparrow$)	-
22/06/10-02/07/10	50	AOD ($\uparrow\downarrow\uparrow$)	-	-	PR ($\downarrow\uparrow\downarrow$)
20/07/11-27/07/11	50	-	H_{1000} ($\downarrow\uparrow\downarrow$)	NO, CO ($\downarrow\uparrow\downarrow$)	RH ($\uparrow\downarrow\uparrow$)
17/08/11-24/08/11	30	O_3 ($\downarrow\uparrow\downarrow$)	-	O_3 ($\uparrow\downarrow\uparrow$) SO_2 ($\downarrow\uparrow\downarrow$)	-
08/09/11-21/09/11	50	-	-	NO_2, NO_X ($\downarrow\uparrow\downarrow$)	TC ($\downarrow\uparrow\downarrow$)
08/10/11-16/10/11	50	-	-	O_3 ($\uparrow\downarrow\uparrow$)	WS ($\uparrow\downarrow\uparrow$)
06/05/12-23/05/12	30	AOD ($\uparrow\downarrow\uparrow$)	H_{500} ($\downarrow\uparrow\uparrow$)	PM_{10} ($\uparrow\downarrow\uparrow$)	TC ($\downarrow\uparrow\uparrow$)
27/05/12-07/06/12	30	-	H_{1000} ($\uparrow\downarrow\downarrow$)	SO_2 ($\uparrow\downarrow\downarrow$)	PR ($\downarrow\uparrow\uparrow$)

AOD: aerosol optical depth; TC: temperature; WS: wind speed; PR: atmospheric pressure; RH: relative humidity.

heterogeneity was observed in PM_{10} concentrations at all stations, however, on average, high concentrations were observed during daytime, when high TC causes an increase in WS. The diurnal trend in meteorological variables was also observed with maximum (minimum) TC observed during 8:00 to 16:00 LT (4:00 to 5:00 LT). It was found that WS increases during afternoon hours.

Monthly variations of air pollutants and meteorological variables are displayed in Figure 5. Monthly high averages of NO_2, NO and NO_x were observed in the warmer months (April, May, June) especially in the IDL station. Monthly fluctuations were observed for NO with high concentrations during spring and winter. The highest O_3 concentrations occurred from May to August, which are the months of high TC. Alghamdi et al. (2014) found that O_3 concentrations strongly follow variations in TC and observed the highest daytime average O_3 concentration in August (86.43 µg m^{-3}) and the lowest in December (46.06 µg m^{-3}).

CO higher (lower) concentrations were observed in May-July (November-February). High concentrations of CO during summer can be attributed to high dispersion of CO due to dry conditions, relatively high wind speeds, and reduced wet scavenging of CO due to a low rainfall rate.

The monthly variations of SO_2 and H_2S exhibited spatial inhomogeneity across the stations. High concentrations of SO_2 were observed for the IDL station,

Atmospheric blocking and dust storm events

Fig. 3. MODIS satellite-based images for an atmospheric blocking event during June 2008 (top row panels), and dust events during March 2009 (middle row panels) and March 2012 (bottom row panels) (see also Fig. 1 and Table II).

however, no clear pattern was observed for the remaining stations. Peak monthly concentrations for H_2S were observed in April-June for the IDL and BNI stations. H_2S concentrations were constant for the ABR and HQL stations. The STA station displayed a different monthly pattern due to high concentrations recorded during May-September in 2008. PM_{10} peak concentrations were observed during February-April, the time period of dust storm activities in the region (Shalaby et al., 2015).

The monthly variations of TC exhibited an increase (decrease) during April-October (November-February). The monthly variations of PR were opposite to those of TC, with lowest PR during June-August. RH and WS averages were relatively constant in all months, with higher RH in the ABR station, located in a coastal area. RF occurred in December-April. Dry conditions prevailed during the rest of the months (Athar, 2015).

3.2 Weekend effect

The weekend effect of air pollutants was computed for all stations using Friday as weekend and Saturday to Thursday as weekdays, following the discussion in section 2.2.2 (Fig. 6). The weekend effect for CO, NO_2, NO and NO_x was observed in all stations where concentrations were higher during weekdays than in weekends, except for the ABR station, which
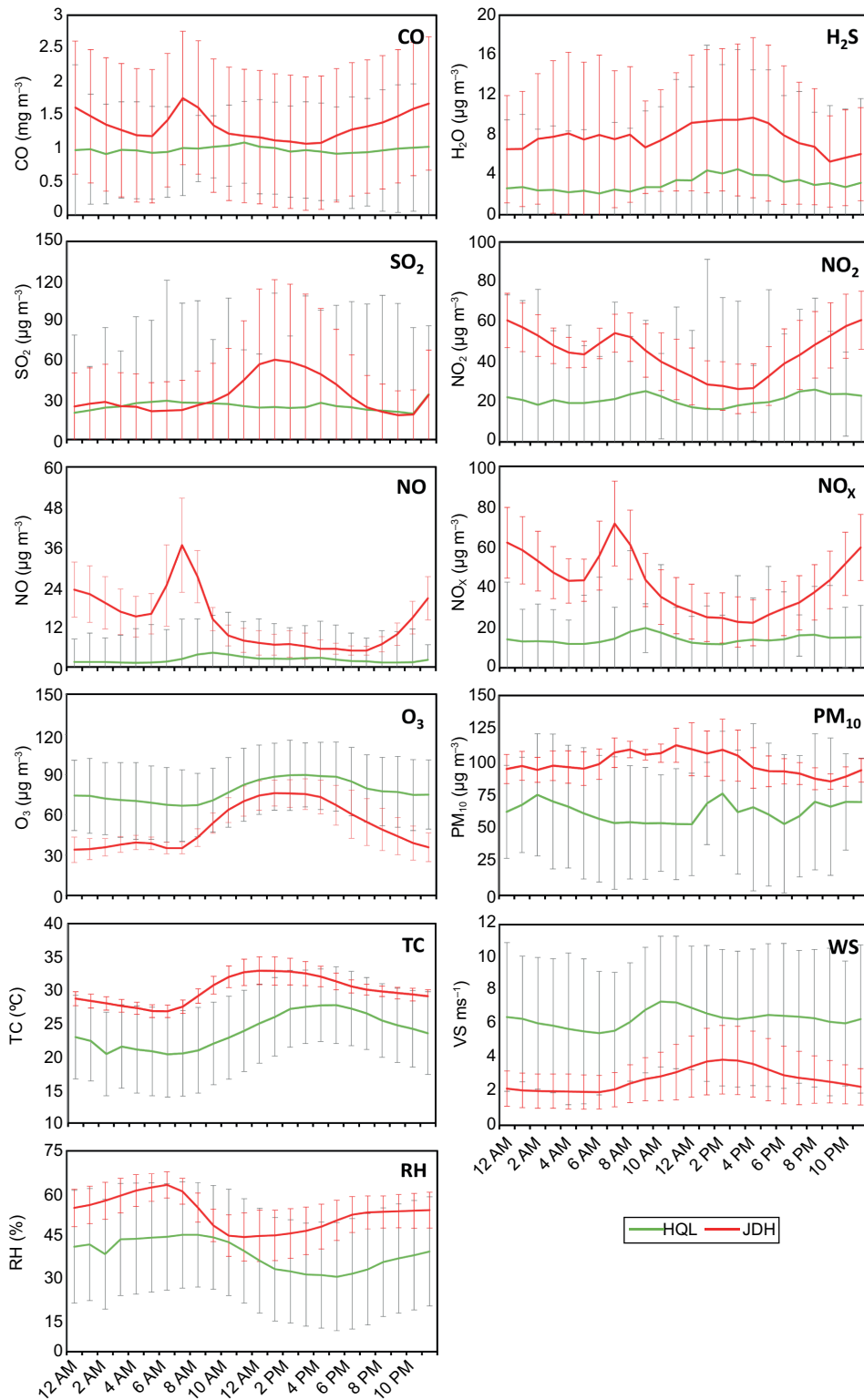
Fig. 4. Hourly variations of air pollutants and meteorological variables for Haqel (HQL) and Jeddah (JDH), including their one sigma standard deviation values, during 2008-2012. JDH shows the average of ABR, STA, BNI and IDL stations values.
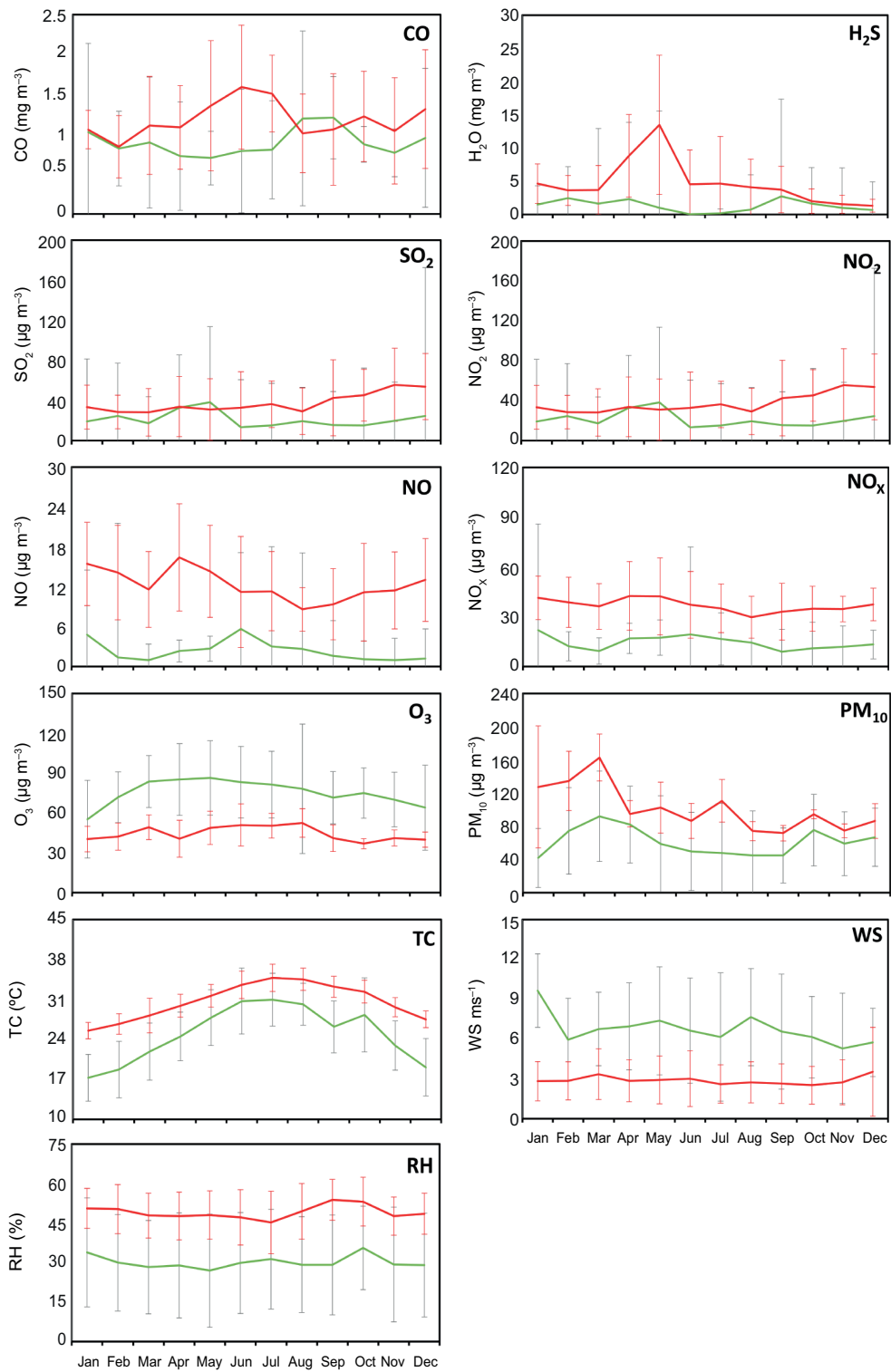
Fig. 5. Same as in Fig. 4 but for a monthly basis.
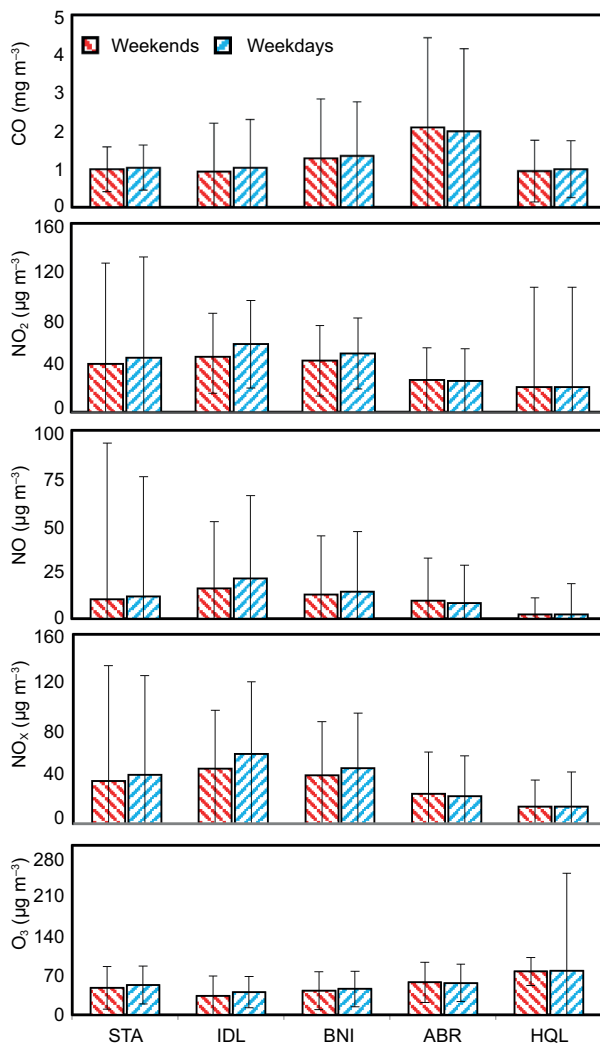
Fig. 6. Weekdays-weekends differences for CO, NO₂, NO and NOx, and O₃ (from top to bottom average concentrations, including their one sigma standard deviation, for each station during 2008-2012.

has high concentration on weekends. The difference between weekends and weekdays was highest at the IDL station.

Low O_3 concentrations on weekdays were detected for all stations except for ABR, where averages for weekdays were greater than weekends. Baidar et al. (2015) reported similar results for California in the USA. The opposite trend was observed for the ABR station due to high vehicular emissions on weekends owing to tourism activities, as this station is located near the shore. High concentrations of O_3 on weekends were recorded since this station had

low NO levels, which indicates that O_3 scavenging from NO was lower, resulting in higher O_3 levels. The weekend effect was not observed for other air pollutants in the region.

O_3 and the NO_x are recognized as pollutants associated to reduced anthropogenic activities on weekends in several regions of the world, such as in California (Qin et al., 2004), Greece (Paschalidou and Kassomenos, 2004), the Iberian Peninsula (Jiménez et al., 2005), southern California (Gao et al., 2005), Japan (Sakamoto et al., 2005), Nepal (Pudasainee et al., 2006), Mexico (Stephens et al., 2008), Egypt (Khoder, 2009), and China (Wang et al., 2014).

3.3 Annual variations
The average NO_2 concentration is decreasing at a rate of –1.97 µg m⁻³ per year ($R^2 = 0.47$). NO and NO_x concentrations are decreasing at rate of –1.73 µg m⁻³ per year ($R^2 = 0.83$), and –2.42 µg m⁻³ per year ($R^2 = 0.63$), respectively. All stations except IDL displayed a decreasing trend, indicating increased NO_x emissions from industries. The increase rate for the IDL station is 11.08 µg m⁻³ per year ($R^2 = 0.73$). The O_3 average concentration for all stations is increasing at a rate of 2.99 µg m⁻³ per year ($R^2 = 0.46$). In Saudi Arabia, this annual increasing rate of O_3 is somewhat higher than that reported for several east Asian countries (Jung et al., 2018) and in Cyprus (Pikridas et al., 2018). The O_3 concentration exhibited an inverse trend with its precursor (NO_x). This behavior was also observed by Mayer (1999), who found that O_3 displayed a long-term increase while a decreasing trend was found for other air pollutants.

The annual CO concentrations of all stations were found to be decreasing at a rate of –0.03 mg m⁻³ per year ($R^2 = 0.62$). Similarly, a decrease in H_2S and SO_2 concentrations is observed. The average trend of H_2S and SO_2 for all stations was –514.91 µg m⁻³ per year ($R^2 = 0.87$) and –6.21 µg m⁻³ per year ($R^2 = 0.89$), respectively.

The PM_{10} average concentration for all stations was found to be increasing at a rate of 9.55 µg m⁻³ per year ($R^2 = 0.65$). The increase in PM_{10} concentrations within the region can be attributed to dust storm events that cause substantial increase in concentrations owing to air pollutant loading (Alghamdi et al., 2015). Dust events in Saudi Arabia occur all

year round with maximum intensity in spring and summer (Shalaby et al., 2015). PM_{10} displays high concentrations during the February-August, since 75% of dust events identified in this study were observed in those months.

3.4 Percentile based changes

The percentiles of O_3 on an hourly time scale showed an increase in all stations except for BNI and HQL (Fig. 7a). An increase in O_3 background values (lower percentiles) was observed in both dry and wet seasons. The behavior of stations BNI and HQL can be attributed to their suburban localization, which implies less sources of air pollutant emissions. High values of solar radiation in summer and during day time lead to higher O_3 concentrations. The higher percentiles of O_3 exhibited relatively large changes; similar changes were observed in its precursors' (NO_2, NO and NO_x) and meteorological variables (TC and WS). High concentrations of O_3 occur in response to an increase in TC and WS (Camalier et al., 2007; Shen and Mickley 2017). The 99th percentile did not exceed the EPA standard of 150 µg m^{-3} for the 3-year period, indicating that O_3 concentrations were within the air quality standard's limit.

The hourly PM_{10} concentrations exhibited an increase in higher percentiles for all stations (Fig. 7b). Increased PM_{10} concentrations were observed at higher percentiles (85th and above) with a similar behavior for WS values. Minimum changes were observed in autumn and the wet season. During summer and the dry seasons, PM_{10} concentrations were observed increasing until the 90th percentile and then decreasing with higher percentiles. In the 1st quartile, the highest concentrations were recorded in spring and summer for most stations. PM_{10} concentrations exceeded the air quality standards values of during summer at the BNI station, where the median value was higher than 150 µg m^{-3} during the second half of the study period.

NO_2, NO and NO_x showed relatively small or no changes in lower percentiles and larger changes in higher percentiles (Fig. 7c). Only one station (BNI) displayed an increase above the 90th percentile for NO_2 and NO_x in winter. The 99th percentile did not exceed the air quality standard of 188 µg m^{-3} for stations STA and HQL in the first half of the study period.

The CO concentration increased in the second half of the study period for all time scales except for the wet season between the 1st to 3rd quartiles; however, a decrease in higher percentiles is observed for all time scales indicating a decrease in occurrence of high CO concentrations (not shown). The value of the 99th percentile in the studied time period was well below the EPA standard of 40 mg m^{-3}.

SO_2 and H_2S concentrations decreased in the second half of the study period for the dry season, contrary to their increase during the wet season for all percentiles (not shown). The 1st, 2nd and 3rd quartiles of SO_2 concentrations did not exceed the USA-EPA 24-h average standard of 365 µg m^{-3}. The H_2S hourly average was compared to the California Ambient Air Quality Standard (due to the unavailability of a USA-EPA air quality standard for H_2S), and daily concentrations were found to be higher than the standard of 45 µg m^{-3} for the STA station during the first half of the study period and for the ABR station in the second half. Values for the median and 3rd quartile exceeded the standard on all stations except ABR, and in the second half exceeded the standard only for ABR station.

The percentile-based changes in meteorological variables provide an insight into the short-term climatology of the region. The lower percentiles for TC, PR and WS decreased in the second half of the study period, while an increase was observed for RH. Conversely, higher percentiles were found increasing (decreasing) for TC, PR and WS (RH). In the wet season, a decrease in TC and PR is observed with an increase in higher percentiles of RH indicating chances of extreme weather events. Percentile based changes on multiple time scales for TC between equal halves (during 2008-2010) are displayed in Fig. 7d.

3.5 Relation of elevated PM_{10} concentration and dust storms

Several short- and long-term case studies carried out in different countries of the East Mediterranean basin found a relationship between dust storms and various indicators of air quality (Ackerman and Cox, 1989; Draxler et al., 2001; Kutiel and Furman, 2003; Zender and Kwon, 2005; Nastos, 2012; Sharma et al., 2012; Gherboudj and Ghedira, 2014). In this study , in situ atmospheric conditions and satellite-based AOD were

O₃
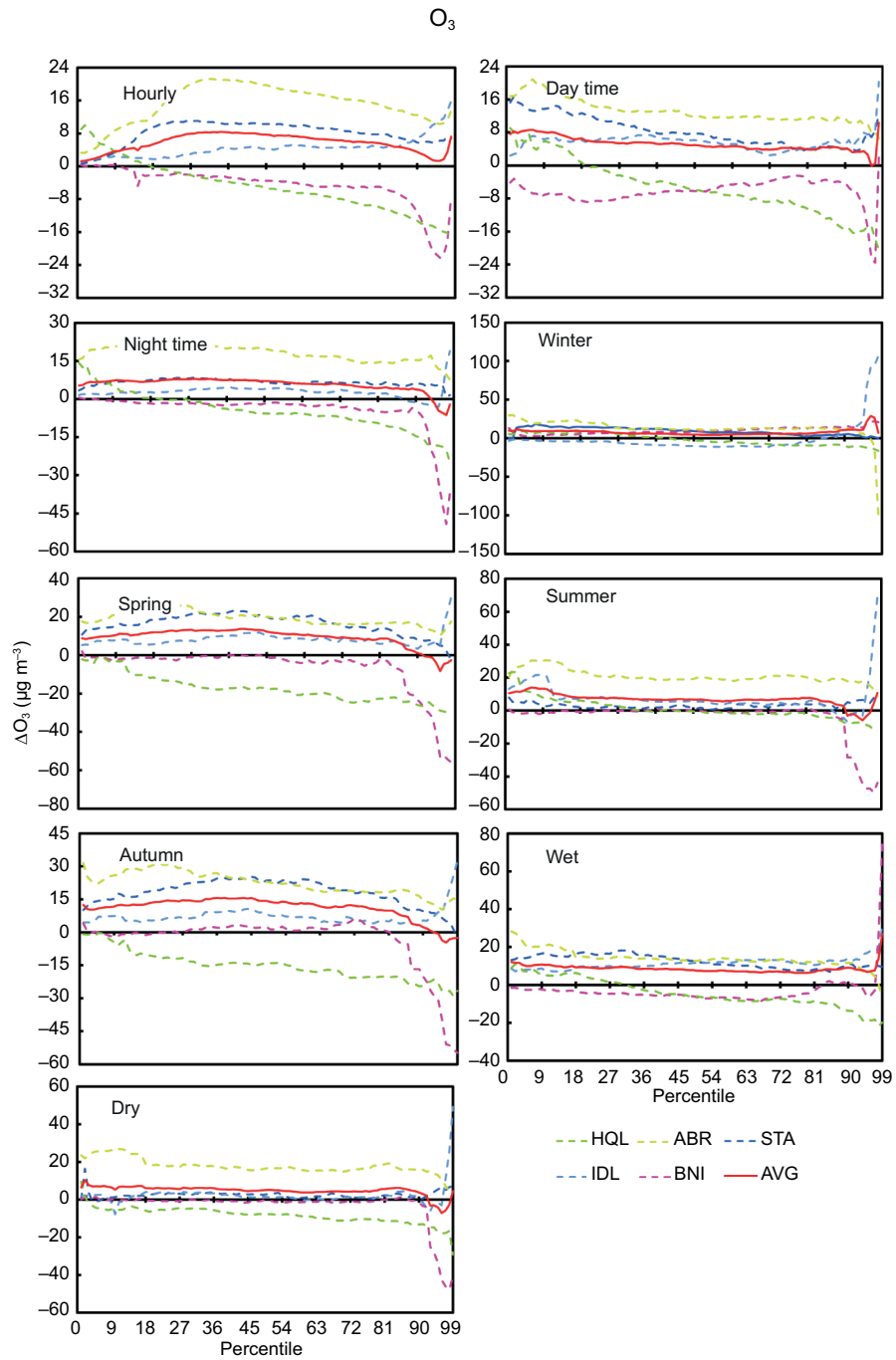
Fig. 7a. Hourly daytime, nighttime and seasonal (winter, spring, summer, autumn, wet and dry) time scale percentile changes for variable O₃ between the two halves of the study period (2008-2012).
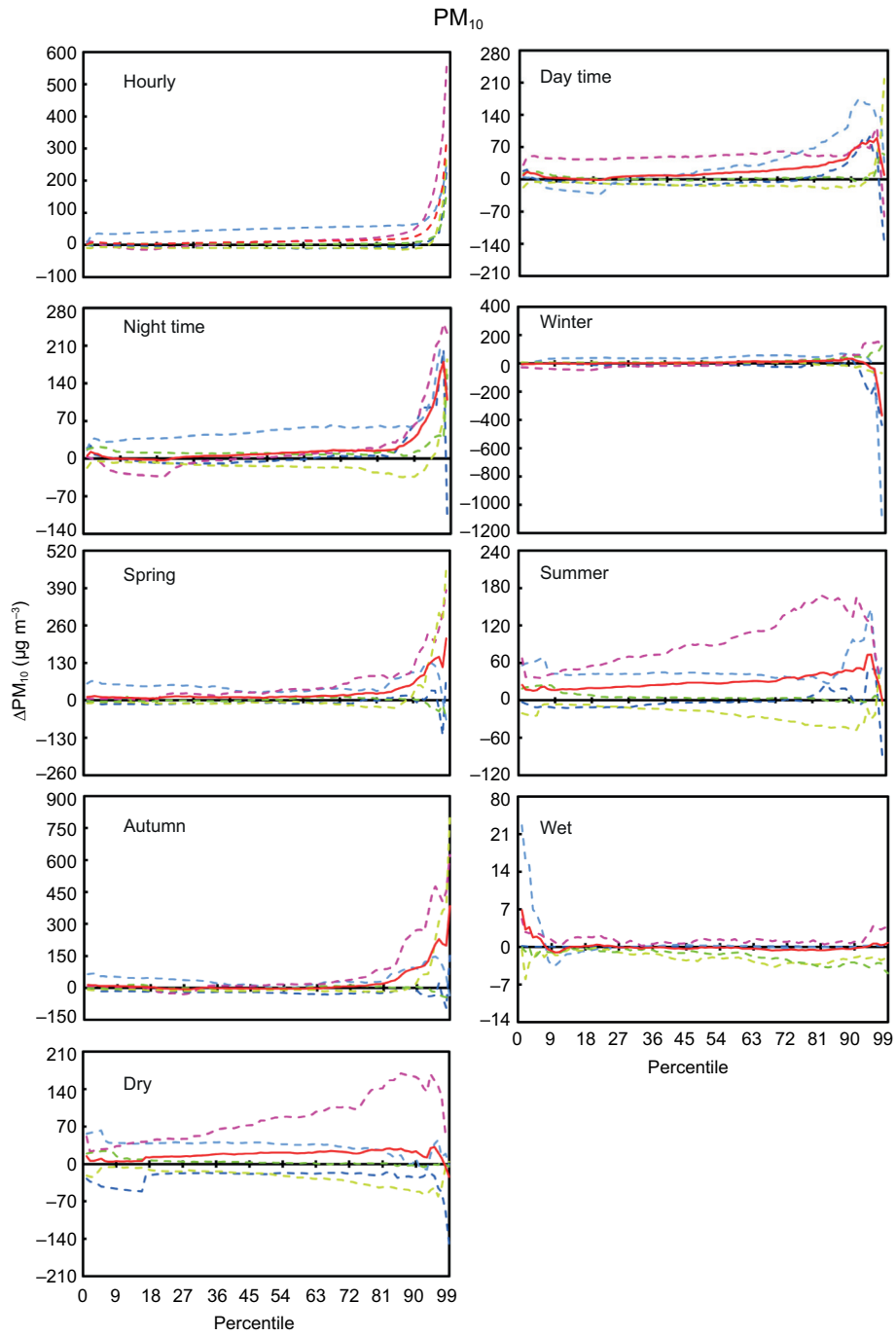
Fig. 7b. Same as Figure 7a but for variable PM_{10}.

NO$_2$
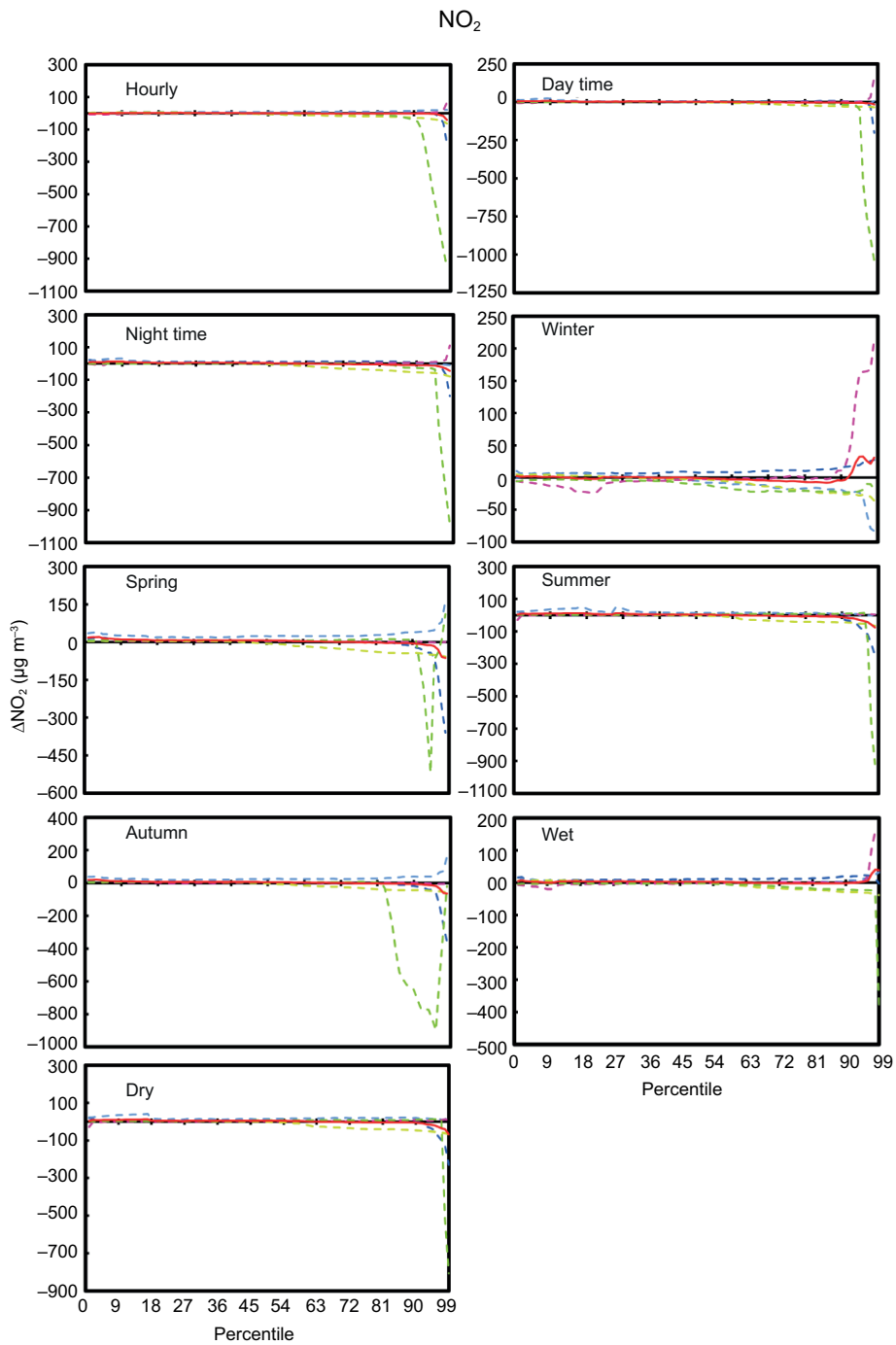
Fig. 7c. Same as Figure 7a but for variable NO$_2$.
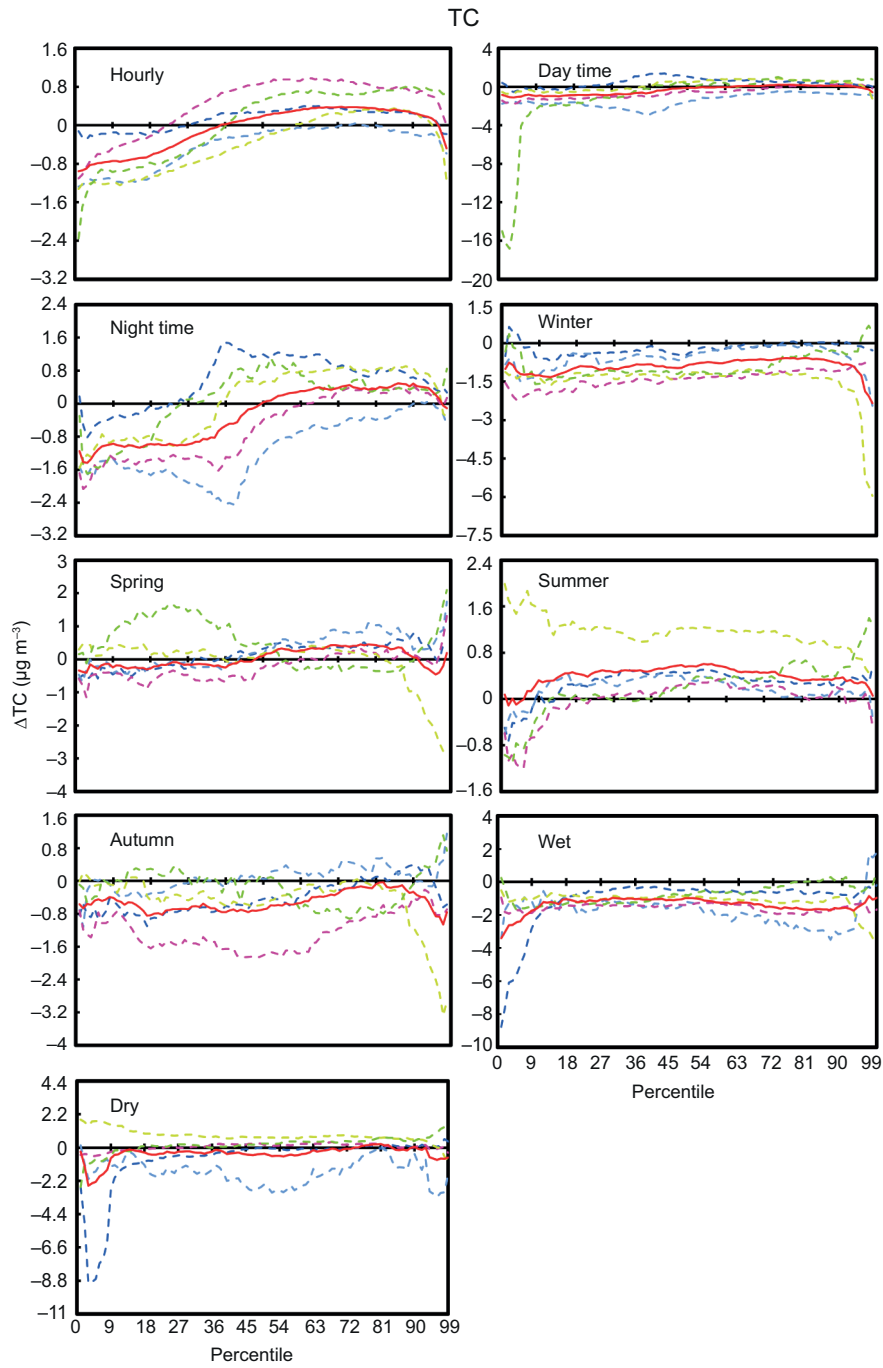
Fig. 7d. Same as Figure 7a but for variable TC.

assessed for a total of 12 events identified in a 5-year period to study the relationship between occurrence of dust storms and modulation of air pollutants in Saudi Arabia. Only eight of these events occurred during spring (February-April). Two of these cyclonic events, both of which were studied earlier, are briefly discussed next as illustrative examples, providing additional complementary information. For details of the remaining six cyclonic events, see Tazeem (2018).

One of the studied events, identified by Alharbi et al. (2013), occurred during March 5 to 14, 2009 (Figs. S2 an S3). The storm was caused by the presence of a cold front with an upper-level jet. Dust storm events are triggered by a low PR trough produced by presence of jet stream in the region (Hermida et al., 2018). The other studied event, which occurred during March 11 to 23, 2012, was analyzed by Prakash et al. (2015), who assessed the impact of dust events on radiation fluxes and local climate characteristics (Figs. S4 and S5). A low PR system was located at 30º to 80º N that resulted in drop of PR, TC and RH and an increase in surface WS, which ranged from 3 to 8 m s^{-1} during the event with essentially a two-peak structure in PM_{10} concentration (Reizer and Juda-Rezler, 2016). Beegum et al. (2018) observed that dust emissions are strongly related to WS, hence accurate meteorological parameters are crucial for dust storm identification and air pollutants simulations. An approximate co-variation of WS and PM_{10} was also noted in Wuhan, China, based on in-situ observations on a daily basis during 2013-2016 (Zhang et al., 2018b). An increase in AOD was also observed with simultaneous increase in PM_{10} concentrations. Maghrabi and Alotaibi (2018) attributed the AOD increase during spring to the impact of dust events. Most of the events observed in the study exhibited a two-peak structure in PM_{10} concentrations. Similar elevated air pollutant concentrations were observed in the remaining six events.

3.6 Blocking impacts on air pollutant concentrations

Anticyclonic atmospheric blockings are events linked with persistent high PR that leads to extreme weather conditions such as heat waves, cold waves and severe air pollution episodes (Sitnov et al., 2017; Sitnov and Mokhov, 2017). Webber et al. (2017) found a strong association between blocking events over western Europe and PM_{10} concentrations over the UK in winter.

In the present study, a total of 26 events were identified, of which 19 occurred during the summer (May-October). Fourteen of these events displayed a significant positive deviation in geopotential height at 500 hPa (H_{500}) from the 5-year mean during blocking periods. Likewise, seven out of the 26 were identified during winter (November-December and February). Six of them displayed significant negative deviation from the 5-year H_{500} mean. In this study, 14 blocking events with positive deviation from the mean were further investigated to identify significant changes in air pollutant concentrations: AOD, O_3, NO_2 and SO_2 as well as H_{500} and geopotential height at 1000 hPa (H_{1000}). It was found that 12 blocking events resulted in significant changes in one or more observed variables (Table II). The main cause of these changes in parameters was found to be associated with high PR development over the study region during the blocking period. The ensuing stagnation in air leads to a decrease in WS (which was identified via in situ observations), giving rise to accumulation of air pollutants in the region.

4. Conclusions

This study presents a detailed investigation of the spatiotemporal variations in air pollutants (CO, SO_2, H_2S, NO_2, NO, NO_x, O_3 and PM_{10}) and their relationships with meteorological variables (RF, RH, PR, TC, WS, and WD) from in-situ observations for a period of five consecutive years (2008 to 2012) using 15 min observations from ground-based data of five stations; one located in city of Haqel (HQL) and four located in city of Jeddah (STA, BNI, IDL and ABR), all in Saudi Arabia. The main conclusions deduced from the study are as follows:

- Most air pollutants displayed a decreasing trend except for PM_{10} and O_3 in the region. The IDL station, located in the industrial area of Jeddah, is the only station that displayed an increase in NO_2, NO and NO_x emissions, indicating excessive release of nitrogen-based oxides.
- High concentrations of NO_2, NO and NO_x were observed during high traffic rush hours (7:00-9:00 LT), whereas the lowest O_3 concentrations were found

at 7:00 LT. A statistically significant correlation was found between WS and O_3 concentration at hourly and diurnal time scales. PM_{10} also disperses in the atmosphere due to high WS. High O_3 concentrations occurred in May-August due to high solar radiation and high WS in summer.

• Due to low WS, there is a greater chance for air pollutants to accumulate. Accumulation of pollutants such as NO can result in reduction of O_3 concentrations and vice versa. Hence, in this study a statistically significant correlation was found between WS and O_3 concentrations at hourly and diurnal time scales.

• A percentile-based analysis showed a decrease in all air pollutants except for O_3, whose lower percentiles were found increasing during the second half of the study period, and PM_{10} values were found increasing in higher percentiles. An increase in O_3 lower percentiles indicates an increase in background values, whereas an increase in PM_{10} higher percentiles indicates an increase in extreme PM_{10} values. The PM_{10} concentration exceeded the USA-EPA air quality standard, while the H_2S concentration exceeded air quality standards in the first half of the study period; however, a decrease was observed in the second half.

• Upper air low pressure systems located at 30º to 80º N cause the drop of PR and TC, and an increase in surface WS, resulting in extreme weather events such as dust storms. During such events, PM_{10} high concentrations greater than 3σ were observed in the study area, relative to non-extreme weather.

• Anticyclonic blocking events resulted in significant changes in air pollutant concentrations during the blocking period due to air stagnation and a decrease in surface WS, which resulted in accumulation of air pollutants.

Acknowledgments

References

Abbass RA, Kumar P, el-Gendy A. 2017. An overview of monitoring and reduction strategies for health and climate change related emissions in the Middle East and North Africa region. Atmospheric Environment 175: 33-43. https://doi.org/10.1016/j.atmosenv.2017.11.061

Ackerman SA, Cox SK. 1989. Surface weather observations of atmospheric dust over the southwest summer monsoon region. Meteorology and Atmospheric Physics. 41: 19-34. https://doi.org/10.1007/BF01032587

Albaqami S. 2019. Spatial and temporal analysis of dust storms in Saudi Arabia and associated impacts, using Geographic Information Systems and remote sensing. Ph.D. thesis. Department of Geography, The University of Exeter, UK. http://hdl.handle.net/10871/40729

Alghamdi MA, Khoder M, Harrison RM, Hyvärinen AP, Hussein T, Al-Jeelani H, Abdelmaksoud AS, Goknil MH, Shabbaj II, Almehmadi FM, Lihavainen H. 2014. Temporal variations of O_3 and NO_x in the urban background atmosphere of the coastal city Jeddah, Saudi Arabia. Atmospheric Environment 94: 205-214. https://doi.org/10.1016/j.atmosenv.2014.03.029

Alghamdi MA, Almazroui M, Shamy M, Redal MA, Alkhalaf AK, Hussein MA, Khoder MI. 2015. Characterization and elemental composition of atmospheric aerosol loads during springtime dust storm in western Saudi Arabia. Aerosol and Air Quality Research 15: 440-453. https://doi.org/10.4209/aaqr.2014.06.0110

Alharbi BH, Maghrabi A, Tapper N. 2013. The March 2009 dust event in Saudi Arabia: Precursor and supportive environment. Bulletin of the American Meteorological Society 94: 515-528. https://doi.org/10.1175/BAMS-D-11-00118.1

Al-Hemoud A, Al-Dousari A, Al-Shatti A, Al-Khayat A, Behbehani W, Malak M. 2018. Health impact assessment associated with exposure to PM_{10} and dust storms in Kuwait. Atmosphere 9: 1-6. https://doi.org/10.3390/atmos9010006

Ali MA, Nichol JE, Bilal M, Qiu Z, Mazhar U, Wahiduzzaman M, Almazroui M, Islam MN. 2020. Classification of aerosols over Saudi Arabia from 2004-2016. Atmospheric Environment 241: 117785. https://doi.org/10.1016/j.atmosenv.2020.117785

Al-Jeelani HA. 2014. Diurnal and seasonal variations of surface ozone and its precursors in the atmosphere of Yanbu, Saudi Arabia. Journal of Environmental Protection 5: 408-422. https://doi.org/10.4236/jep.2014.55044

Alvarado MJ, McVey AE, Hegarty JD, Cross ES, Hasen-kopf CA, Lynch R, Kennelly EJ, Onasch TB, Awe Y, Sanchez-Triana E, Kleiman G. 2019. Evaluating the use of satellite observations to supplement ground-level air quality data in selected cities in low-and middle-income countries. Atmospheric Environment 218: 117016. https://doi.org/10.1016/j.atmosenv.2019.117016

Amsalu E, Guo Y, Li H, Wang T, Liu Y, Wang T, Liu Y, Wang A, Tao L, Liu X, Luo Y, Tao L, Luo Y, Zhang F, Yang X, Li X, Wang W, Guo X. 2019. Short-term effect of ambient sulfur dioxide (SO_2) on cause-specific cardiovascular hospital admission in Beijing, China: a time series study. Atmospheric Environment 208: 74-81. https://doi.org/10.1016/j.atmosenv.2019.03.015

Athar H. 2014. Trends in observed extreme climate indices in Saudi Arabia during 1979 2008. International Journal of Climatology 34: 1561-1574. https://doi.org/10.1002/joc.3783

Athar H. 2015. Teleconnections and variability in observed rainfall over Saudi Arabia during 1978-2010. Atmospheric Science Letters 16: 373-379. https://doi.org/10.1002/asl2.570

Baidar S, Hardesty RM, Kim SW, Langford AO, Oetjen H, Senff CJ, Volkamer R. 2015. Weakening of the weekend ozone effect over California's South Coast Air Basin. Geophysical Research Letters 42: 9457-9464. https://doi.org/10.1002/2015GL066419

Beegum SN, Gherboudj I, Chaouch N, Temimi M, Ghedira H. 2018. Simulation and analysis of synoptic scale dust storms over the Arabian Peninsula. Atmospheric Research 199: 62-81. https://doi.org/10.1016/j.atmosres.2017.09.003

Brauer M, Guttikunda SK, Nishad KA, Dey S, Tripathi SN, Weagle C, Martin RV. 2019. Examination of monitoring approaches for ambient air pollution: a case study for India. Atmospheric Environment 216: 116940. https://doi.org/10.1016/j.atmosenv.2019.116940

Camalier L, Cox W, Dolwick P. 2007. The effects of meteorology on ozone in urban areas and their use in assessing ozone trends. Atmospheric Environment 41: 7127-7137. https://doi.org/10.1016/j.atmosenv.2007.04.061

Draxler RR, Gillette DA, Kirkpatrick JS, Heller J. 2001. Estimating PM_{10} air concentrations from dust storms in Iraq, Kuwait and Saudi Arabia. Atmospheric Environment 35: 4315-4330. https://doi.org/10.1016/S1352-2310(01)00159-5

Engel-Cox JA, Hoff RM, Haymet ADJ. 2004. Recommendations on the use of satellite remote-sensing data for urban air quality. Journal of the Air and Waste Management 54: 1360-1371. https://doi.org/10.1080/10473289.2004.10471005

Gao OH, Holmén BA, Niemeier DA. 2005. Nonparametric factorial analysis of daily weigh-in-motion traffic: implications for the ozone "weekend effect" in Southern California. Atmospheric Environment 39: 1669-1682. https://doi.org/10.1016/j.atmosenv.2004.11.028

Gherboudj I, Ghedira H. 2014. Spatiotemporal assessment of dust loading over the United Arab Emirates. International Journal of Climatology 34: 3321-3335. https://doi.org/10.1002/joc.3909

Hassan IA, Basahi JM, Ismail IM, Habeebullah TM. 2013. Spatial distribution and temporal variation in ambient ozone and its associated NOx in the atmosphere of Jeddah City, Saudi Arabia. Aerosol and Air Quality Research 13: 1712-1722. https://doi.org/10.4209/aaqr.2013.01.0007

Hermida L, Merino A, Sánchez JL, Fernández-González S, García-Ortega E, López L. 2018. Characterization of synoptic patterns causing dust outbreaks that affect the Arabian Peninsula. Atmospheric Research 199: 29-39. https://doi.org/10.1016/j.atmosres.2017.09.004

Hidy GM. 2019. Atmospheric aerosols: some highlights and highlighters, 1950 to 2018. Aerosol Science and Engineering 3: 1-20. https://doi.org/10.1007/s41810-019-00039-0

Hinds WC. 1999. Aerosol technology: properties, behavior, and measurement of airborne particles. Wiley, New York, 1999.

IPCC. 2014. Climate Change 2014: Impacts, adaptation, and vulnerability. Part B: Regional aspects. Contribution of Working Group II to the Fifth Assessment Report of the Intergovernmental Panel on Climate Change (Field CB, Barros VR, Dokken DJ, Mach KJ, Mastrandrea MD, Bilir TE, Chatterjee M, Ebi KL, Estrada YO, Genova RC, Girma B, Kissel ES, Levy AN, MacCracken S, Mastrandrea PR, White LL, Eds.). Cambridge University Press, United Kingdom and New York, NY, USA, 688 pp.

IPCC. 2021. Climate Change 2021: The Physical Science Basis. Contribution of Working Group I to the Sixth Assessment Report of the Intergovernmental Panel on Climate Change (Masson-Delmotte V, Zhai P, Pirani A, Connors SL, Péan C, Berger S, Caud N, Chen Y,

Goldfarb L, Gomis MI, Huang M, Leitzell K, Lonnoy E, Matthews JBR, Maycock TK, Waterfield T, Yelekçi O, Yu R, Zhou B, Eds.). In Press.

Iqbal MF, Athar H. 2018. Variability, trends, and teleconnections of observed precipitation over Pakistan. Theoretical and Applied Climatology 134: 613-632. https://doi.org/10.1007/s00704-017-2296-1

Jiménez P, Parra R, Gassó S, Baldasano JM. 2005. Modeling the ozone weekend effect in very complex terrains: a case study in the northeastern Iberian Peninsula. Atmospheric Environment 39: 429-444. https://doi. org/10.1016/j.atmosenv.2004.09.065

Jung HC, Moon BK, Wie J. 2018. Seasonal changes in surface ozone over South Korea. Heliyon 4: e00515. https://doi.org/10.1016/j.heliyon.2018.e00515

Kalnay E, Kanamitsu M, Kistler R, Collins W, Deaven D, Gandin L, Iredell M, Saha S, White G, Woollen J, Zhu Y, Chelliah M, Ebisuzaki W, Higgins W, Janowiak J, Mo KC, C. Ropelewski C, Wang J, Leetmaa A, Reynolds R, Jenne R, Joseph D. 1996. The NCEP/ NCAR 40-year reanalysis project, Bulletin of American Meteorological Society 77: 437-470. https://doi. org/10.1175/1520-0477(1996)077<0437:TNYRP>2.0. CO;2

Kaufman YJ, Tanré D, Remer LA, Vermote EF, Chu A, Holben BN. 1997. Operational remote sensing of tropospheric aerosol over land from EOS moderate resolution imaging spectroradiometer. Journal of Geophysical Research: Atmospheres 102: 17051-17067. https://doi.org/10.1029/96JD03988

Kedia S, Ramachandran S. 2009. Variability in aerosol optical and physical characteristics over the Bay of Bengal and the Arabian Sea deduced from Ångström exponents. Journal of Geophysical Research Atmospheres 114: D14207. https://doi.org/10.1029/2009JD011950

Khoder MI. 2009. Diurnal, seasonal and weekdays-weekends variations of ground level ozone concentrations in an urban area in greater Cairo. Environmental Monitoring and Assessment 149: 349-362. https://doi. org/10.1007/s10661-008-0208-7

Kumar KR, Attada R, Dasari HP, Vellore RK, Langdon S, Abualnaja YO, Hoteit I. 2018. Aerosol Optical Depth variability over the Arabian Peninsula as inferred from satellite measurements. Atmospheric Environment 187: 346-357. https://doi.org/10.1016/j. atmosenv.2018.06.011

Kutiel H, Furman HK. 2003. Dust storms in the Middle East: sources of origin and their temporal characteristics. Indoor and Built Environment 12: 419-426. https://doi. org/10.1177/1420326X03037110

Li J, Chen H, Li X, Wang M, Zhang X, Cao J, Shen F, Wu Y, Xu S, Fan H, Da G., Huang R-j, Wang J, Chan CK, Jesus ALD, Morawska L, Yao M. 2019. Differing toxicity of ambient particulate matter (PM) in global cities. Atmospheric Environment 212: 305-315. https:// doi.org/10.1016/j.atmosenv.2019.05.048

Lihavainen H, Alghamdi MA, Hyvärinen A, Hussein T, Neitola K, Khoder M, Abdelmaksoud AS, Al-Jeelani H, Shabbaj II, Almehmadi FM. 2017. Aerosol optical properties at rural background area in Western Saudi Arabia. Atmospheric Research 197: 370-378. https:// doi.org/10.1016/j.atmosres.2017.07.019

Lihavainen H, Alghamdi MA, Hyvärinen AP, Hussein T, Aaltonen V, Abdelmaksoud AS, Al-Jeelani H, Almazroui M, Almehmadi FM, Al-Zawad FM, Hakala J. 2016. Aerosols physical properties at Hada Al Sham, western Saudi Arabia. Atmospheric Environment 135: 109-117. https://doi.org/10.1016/j. atmosenv.2016.04.001

Luo D, Zhang W. 2020. A Nonlinear Multiscale Theory of Atmospheric Blocking: Dynamical and Thermodynamic Effects of Meridional Potential Vorticity Gradient. Journal of Atmospheric Sciences 77: 2471-2500. https://doi.org/10.1175/JAS-D-20-0004.1

Maghrabi AH, Al-Dosari AF. 2016. Effects on surface meteorological parameters and radiation levels of a heavy dust storm occurred in Central Arabian Peninsula. Atmospheric Research 182: 30-35. https://doi. org/10.1016/j.atmosres.2016.07.024

Maghrabi AH, Alotaibi RN. 2018. Long-term variations of AOD from an AERONET station in the central Arabian Peninsula. Theoretical and Applied Climatology 134: 1015-1026. https://doi.org/10.1007/s00704-017-2328-x

Mallik C, Mahapatra PS, Kumar P, Panda S, Boopathy R, Das T, Lal S. 2019. Influence of regional emissions on SO$_2$ concentrations over Bhubaneswar, a capital city in eastern India downwind of the Indian SO$_2$ hotspots. Atmospheric Environment 209: 220-232. https://doi. org/10.1016/j.atmosenv.2019.04.006

Martin RV. 2008. Satellite remote sensing of surface air quality. Atmospheric Environment 42: 7823-7843. https://doi.org/10.1016/j.atmosenv.2008.07.018

Mayer H. 1999. Air pollution in cities. Atmospheric Environment 33: 4029-4037. https://doi.org/10.1016/ S1352-2310(99)00144-2

Mora M, Braun RA, Shingler T, Sorooshian A. 2017. Analysis of remotely-sensed and surface data of aerosols and meteorology for the Mexico megalopolis area between 2003 and 2015. Journal of Geophysical Research: Atmospheres 122: 8705-8723. https://doi.org/10.1002/2017JD026739

Namdari S, Karimi N, Sorooshian A, Mohammadi G, Sehatkashani S. 2018. Impacts of climate and synoptic fluctuations on dust storm activity over the Middle East. Atmospheric Environment 173: 265-276. https://doi.org/10.1016/j.atmosenv.2017.11.016

NASEM. 2016. The future of atmospheric chemistry research: remembering yesterday, understanding today, anticipating tomorrow. National Academies of Sciences, Engineering, and Medicine. The National Academies Press Washington, DC, USA.

Nastos PT. 2012. Meteorological patterns associated with intense Saharan dust outbreaks over Greece in winter. Advances in Meteorology 2012: 828301. https://doi.org/10.1155/2012/828301

Ordóñez C, Barriopedro D, García-Herrera R. 2019. Role of the position of the north Atlantic jet in the variability and odds of extreme PM_{10} in Europe. Atmospheric Environment 210: 35-46. https://doi.org/10.1016/j.atmosenv.2019.04.045

Paschalidou AK, Kassomenos PA. 2004. Comparison of air pollutant concentrations between weekdays and weekends in Athens, Greece for various meteorological conditions. Environmental Technology 25: 1241-1255. https://doi.org/10.1080/09593332508618372

Peeples L. 2020. How air pollution threatens brain health. Proceedings of National Academy of Sciences 117: 13856-13860. https://doi.org/10.1073/pnas.2008940117

Pikridas M, Vrekoussis M, Sciare J, Kleanthous S, Vasiliadou E, Kizas C, Savvides C, Mihalopoulos N. 2018. Spatial and temporal (short and long-term) variability of submicron, fine and sub-10 μm particulate matter (PM_1, $PM_{2.5}$, PM_{10}) in Cyprus. Atmospheric Environment 191: 79-93. https://doi.org/10.1016/j.atmosenv.2018.07.048

Pinder RW, Klopp JM, Kleiman G, Hagler GS, Awe Y, Terry S. 2019. Opportunities and challenges for filling the air quality data gap in low-and middle-income countries. Atmospheric Environment 215: 116794. https://doi.org/10.1016/j.atmosenv.2019.06.032

Pöschl U. 2005. Atmospheric aerosols: composition, transformation, climate and health effects. Angewandte Chemie International Edition 44: 7520-7540. https://doi.org/10.1002/anie.200501122

Prakash JP, Stenchikov GL, Kalenderski S, Osipov S, Bangalath HK. 2015. The impact of dust storms on the Arabian Peninsula and the Red Sea. Atmospheric Chemistry and Physics 15: 199-222. https://doi.org/10.5194/acp-15-199-2015

Pudasainee D, Sapkota B, Shrestha ML, Kaga A, Kondo A, Inoue Y. 2006. Ground level ozone concentrations and its association with NOx and meteorological parameters in Kathmandu valley, Nepal. Atmospheric Environment 40: 8081-8087. https://doi.org/10.1016/j.atmosenv.2006.07.011

Qin Y, Tonnesen GS, Wang Z. 2004. One-hour and eight-hour average ozone in the California South Coast air quality management district: trends in peak values and sensitivity to precursors. Atmospheric Environment 38: 2197-2207. https://doi.org/10.1016/j.atmosenv.2004.01.010

Raes F, Van Dingenen R, Vignati E, Wilson J, Putaud JP, Seinfeld JH, Adams P. 2000. Formation and cycling of aerosols in the global troposphere. Atmospheric Environment 34: 4215-4240. https://doi.org/10.1016/S1352-2310(00)00239-9

Rahman A, Luo C, Khan MH, Ke J, Thilakanayaka V, Kumar S. 2019. Influence of atmospheric $PM_{2.5}$, PM_{10}, O_3, CO, NO_2, SO_2, and meteorological factors on the concentration of airborne pollen in Guangzhou, China. Atmospheric Environment 212: 290-304. https://doi.org/10.1016/j.atmosenv.2019.05.049

Raizenne M, Neas LM, Damokosh AL, Dockery DW, Spengler JD, Koutrakis P, Ware JH, Speizer FE. 1996. Health effects of acid aerosols on north American children: pulmonary function. Environmental Health Perspectives 104: 559-579. https://doi.org/10.1289/ehp.96104506

Ramanathan V, Crutzen PJ, Lelieveld J, Mitra AP, Althausen D, Anderson J, Andreae MO, Cantrell W, Cass GR, Chung CE, Clarke AD, Coakley JA, Collins WD, Conant WC, Dulac F, Heintzenberg TMJ, Heymsfield AJ, Holben B, Howell S, Hudson J, Jayaraman A, Kiehl JT, Krishnamurti TN, Lubin D, McFarquhar G, Novakov T, Ogren JA, Podgorny IA, Prather K, Priestley K, Prospero JM, Quinn PK, Rajeev K, Rasch P, Rupert S, Sadourny R, Satheesh SK, Shaw GE, Sheridan P, Valero FPJ. 2001. Indian Ocean Experiment: An integrated analysis of the climate forcing and effects of the great Indo-Asian haze. Journal of Geophysical

Research: Atmospheres 106: 28371-28398. https://doi.org/10.1029/2001JD900133

Reizer M, Juda-Rezler K. 2016. Explaining the high PM_{10} concentrations observed in Polish urban areas. Air Quality Atmosphere and Health 9: 517-531. https://doi.org/10.1007/s11869-015-0358-z

Romano S, Perrone MR, Becagli S, Pietrogrande MC, Russo M, Caricato R, Lionetto MG. 2020. Ecotoxicity, genotoxicity, and oxidative potential tests of atmospheric PM_{10} particles. Atmospheric Environment 221: 117085. https://doi.org/10.1016/j.atmosenv.2019.117085

Sakamoto M, Yoshimura A, Kosaka H, Hiraki T. 2005. Study on weekend weekday differences in ambient oxidant concentrations in Hyogo prefecture. Journal of Japan Society for Atmospheric Environment 40: 201-208. https://doi.org/10.11298/taiki1995.40.5_201

Shalaby A, Rappenglueck B, Eltahir EAB. 2015. The climatology of dust aerosol over the Arabian Peninsula. Atmospheric Chemistry and Physics Discussion 15: 1523-1571. https://doi.org/10.5194/acpd-15-1523-2015

Sharma D, Singh D, Kaskaoutis DG. 2012, Impact of two intense dust storms on aerosol characteristics and radiative forcing over Patiala, northwestern India. Advances in Meteorology. 2012: 956814. https://doi.org/10.1155/2012/956814

Shen L, Mickley LJ. 2017. Seasonal prediction of US summertime ozone using statistical analysis of large-scale climate patterns. Proceedings of the National Academy of Sciences 114: 2491-2496. https://doi.org/10.1073/pnas.1610708114

Sitnov SA, Mokhov II. 2017. Formaldehyde and nitrogen dioxide in the atmosphere during summer weather extremes and wildfires in European Russia in 2010 and Western Siberia in 2012. International Journal of Remote Sensing 38: 4086-4106. https://doi.org/10.1080/01431161.2017.1312618

Sitnov SA, Mokhov II, Lupo AR. 2017. Ozone, water vapor, and temperature anomalies associated with atmospheric blocking events over Eastern Europe in spring-summer 2010. Atmospheric Environment 164: 180-194. https://doi.org/10.1016/j.atmosenv.2017.06.004

Soleimani Z, Teymouri P, Boloorani AD, Mesdaghinia A, Middleton N, Griffin DW. 2020. An overview of bioaerosol load and health impacts associated with dust storms: a focus on the Middle East. Atmospheric Environment 223: 117187. https://doi.org/10.1016/j.atmosenv.2019.117187

Sowden M, Mueller U, Blake D. 2018. Review of surface particulate monitoring of dust events using geostationary satellite remote sensing. Atmospheric Environment 183: 154-164. https://doi.org/10.1016/j.atmosenv.2018.04.020

Stephens S, Madronich S, Wu F, Olson JB, Ramos R, Retama A, Munoz R. 2008. Weekly patterns of México City's surface concentrations of CO, NO_x, PM_{10} and O_3 during 1986-2007. Atmospheric Chemistry and Physics 8: 5313-5325. https://doi.org/10.5194/acp-8-5313-2008

Stirnberg R, Cermak J, Fuchs J, Andersen H. 2020. Mapping and understanding patterns of air quality using satellite data and machine learning. Journal of Geophysical Research: Atmospheres 125: e2019JD031380. https://doi.org/10.1029/2019JD031380

Tawabini BS, Lawal TT, Shaibani A, Farahat AM. 2017. Morphological and chemical properties of particulate matter in the Dammam metropolitan region: Dhahran, Khobar, and Dammam, Saudi Arabia. Advances in Meteorology 2017: 8512146. https://doi.org/10.1155/2017/8512146

Tazeem SB. 2018. Spatio-temporal variations of aerosols and meteorological variables for Haqel and Jeddah, Saudi Arabia during 2008-2012. M.Sc. dissertation. Department of Meteorology, COMSATS University Islamabad, Pakistan.

Tomasi C, Fuzzi S, Kokhanovsky A, eds. 2017. Atmospheric aerosols: Life cycles and effects on air quality and climate. John Wiley & Sons, 704 pp.

Vincent P. 2008. Saudi Arabia: An environmental overview. Taylor and Francis, London, 332 pp. https://doi.org/10.1201/9780203030882

Wang YH, Hu B, Ji DS, Liu ZR, Tang GQ, Xin JY, Zhang HX, Song T, Wang LL, Gao WK, Wang XK. 2014. Ozone weekend effects in the Beijing-Tianjin-Hebei metropolitan area, China. Atmospheric Chemistry and Physics 14: 2419-2429. https://doi.org/10.5194/acp-14-2419-2014

Webber CP, Dacre HF, Collins WJ, Masato G. 2017. The dynamical impact of Rossby wave breaking upon UK PM_{10} concentration. Atmospheric Chemistry and Physics 17: 867-881. https://doi.org/10.5194/acp-17-867-2017

Wilks DS. 2020. Statistical methods in the atmospheric sciences. 4th ed. Elsevier,

Woollings T, Barriopedro D, Methven J, Son SW, Martius O, Harvey B, Seneviratne S. 2018. Blocking and its response to climate change. Current Climate Change Reports 4: 287-300. https://doi.org/10.1007/s40641-018-0108-z

Yu Y, Notaro M, Liu Z, Kalashnikova O, Alkolibi F, Fadda E, Bakhrjy F. 2013. Assessing temporal and spatial variations in atmospheric dust over Saudi Arabia through satellite, radiometric, and station data. Journal of Geophysical Research: Atmospheres 118: 13253-13264. https://doi.org/10.1002/2013JD020677

Zender CS, Kwon EY. 2005. Regional contrasts in dust emission responses to climate. Journal of Geophysical Research: Atmospheres 110: D13201. https://doi.org/10.1029/2004JD005501

Zhang B, Jiao L, Xu G, Zhao S, Tang X, Zhou Y, Gong C. 2018a. Influences of wind and precipitation on different-sized particulate matter concentrations ($PM_{2.5}$, PM_{10}, $PM_{2.5-10}$). Meteorology and Atmospheric Physics 130: 383-392. https://doi.org/10.1007/s00703-017-0526-9

Zhang L, Liu Y, Zhao F. 2018b. Important meteorological variables for statistical long-term air quality prediction in eastern China. Theoretical and Applied Climatology 134: 25-36. https://doi.org/10.1007/s00704-017-2245-z

Supplementary material
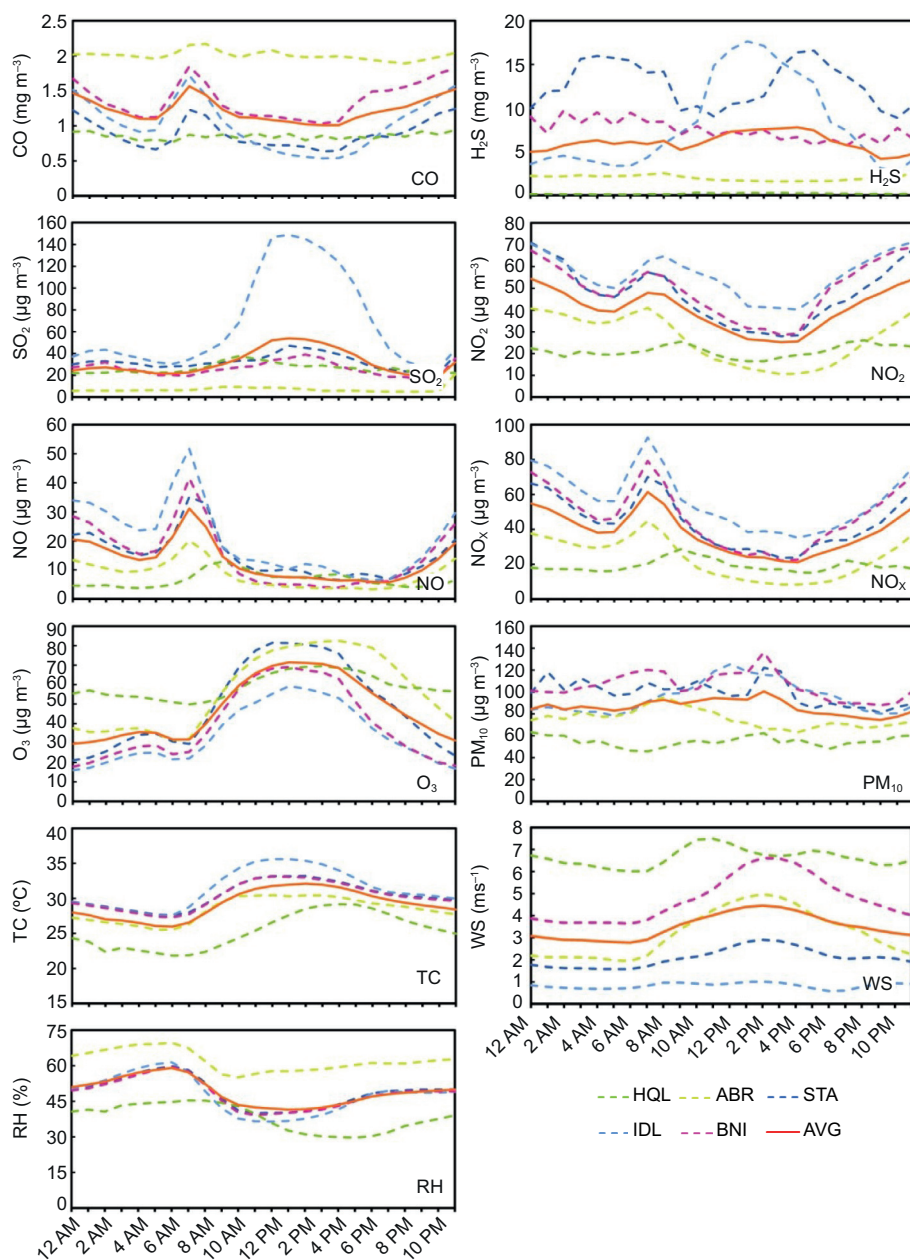
Fig. S1. Hourly variations of air pollutants and meteorological variables for all stations during 2008-2012.
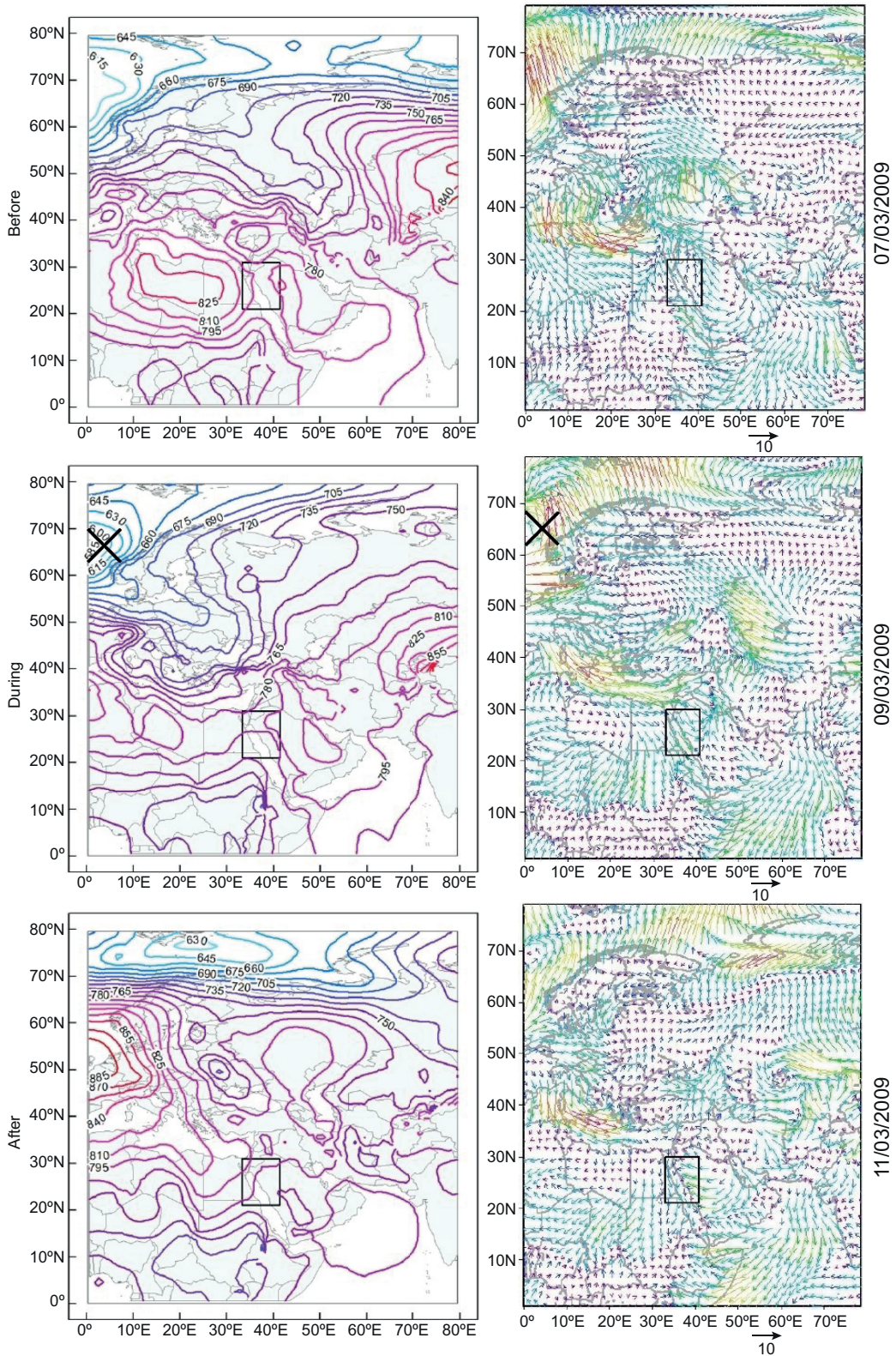
Fig. S2. Left column panels display the AIRS based H925 (m) before, during and after the extreme event (left column panels). The considered duration of the event is from March 5 to 14, 2009. Right column panels display the horizontal 10 m wind distribution derived using the NCEP reanalysis daily averages data. The peak day of the extreme event (09/03/2009) in the middle panel is compared with days before and after. In the right middle panel, the cross marks the center of the low-pressure system. See also Fig. 1.
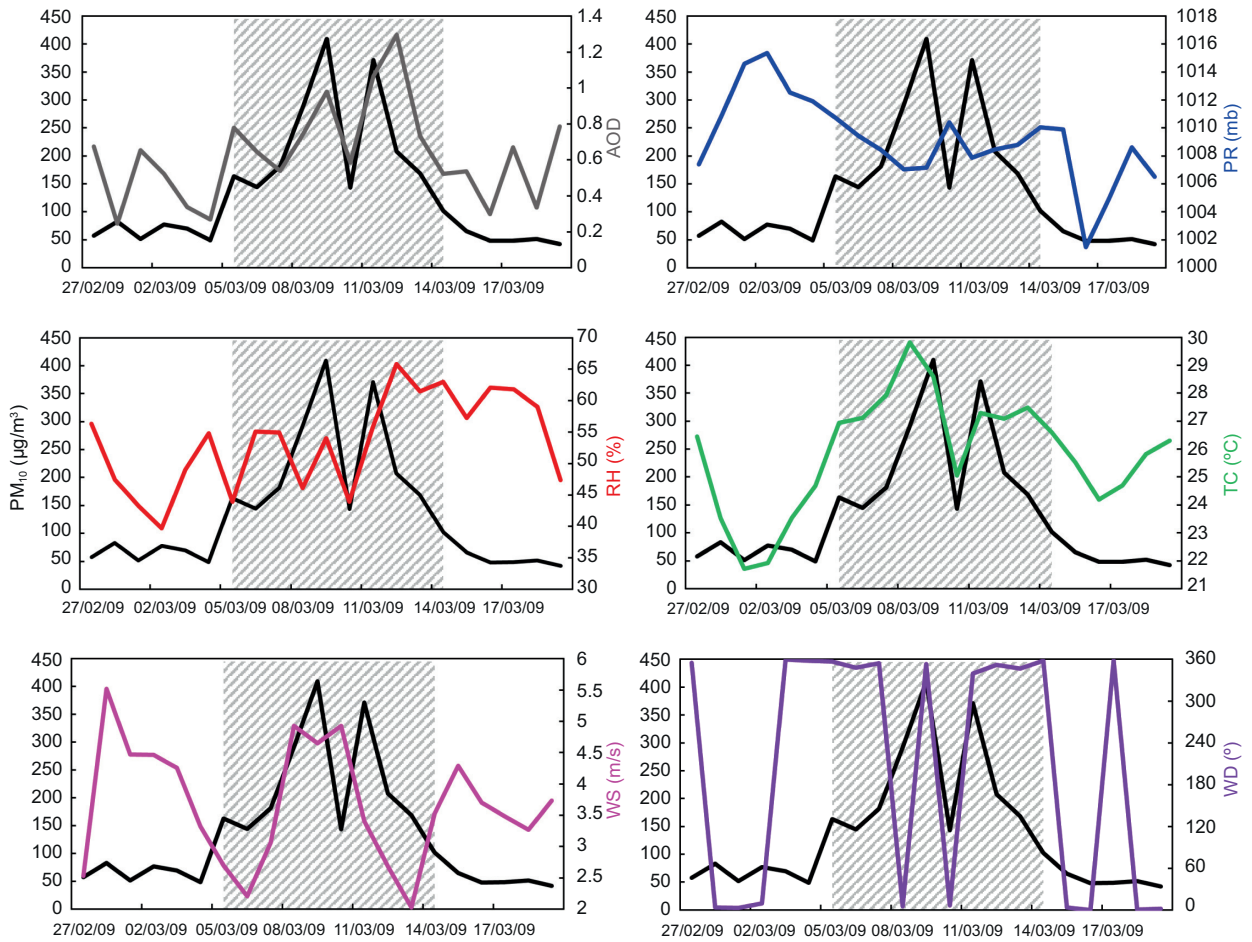
Fig. S3. Covariations of PM$_{10}$ relative to AOD at 442 nm is displayed in top left panel, with PR in top right panel, and other meteorological parameters in next two row panels (RH, TC, RH, WS and WD). The hatched region in each panel refers to the duration of the event displayed in Fig. S2.
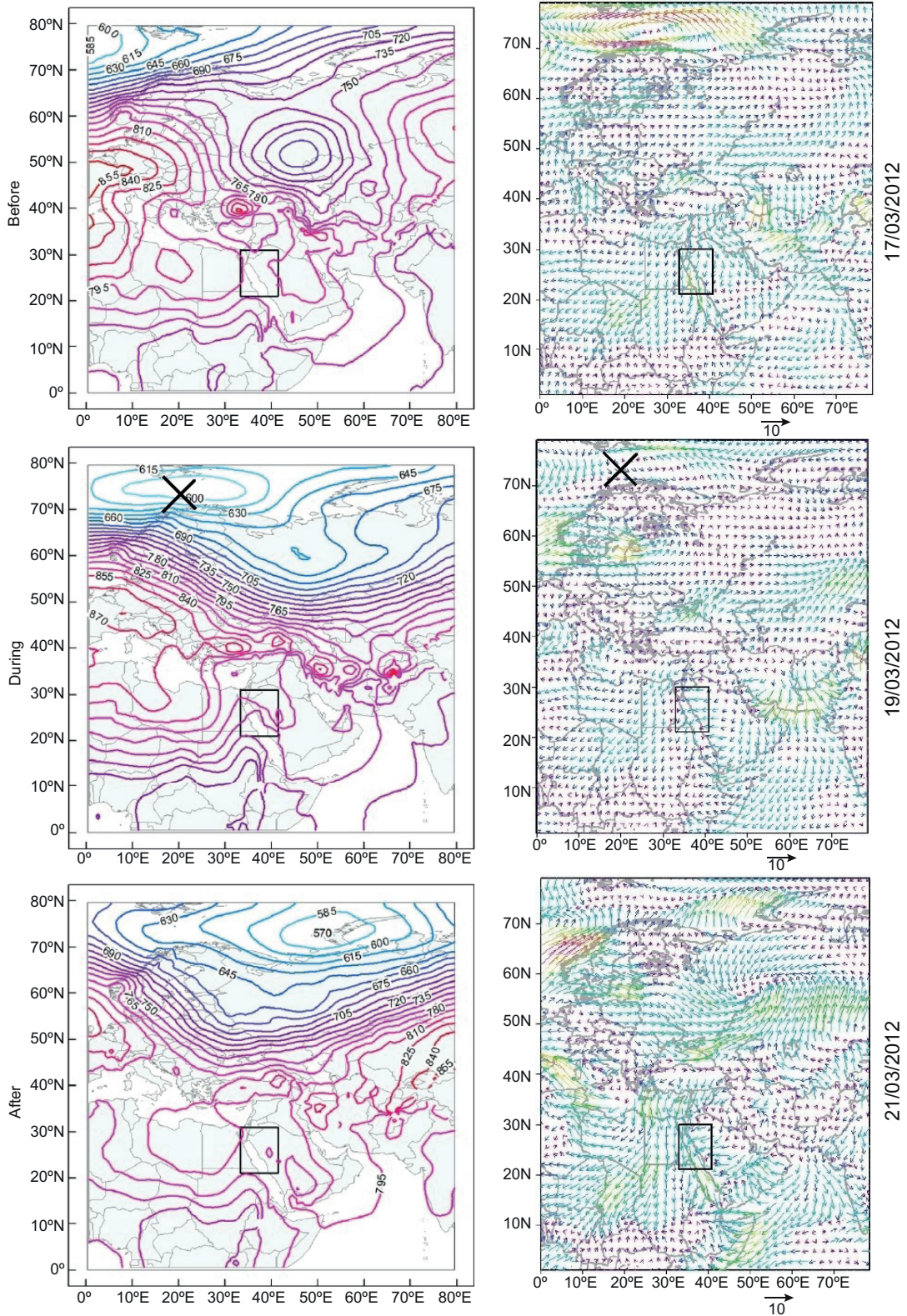
Fig. S4. Same as in Fig. S2, but for the extreme event on March 11 to 23, 2012.
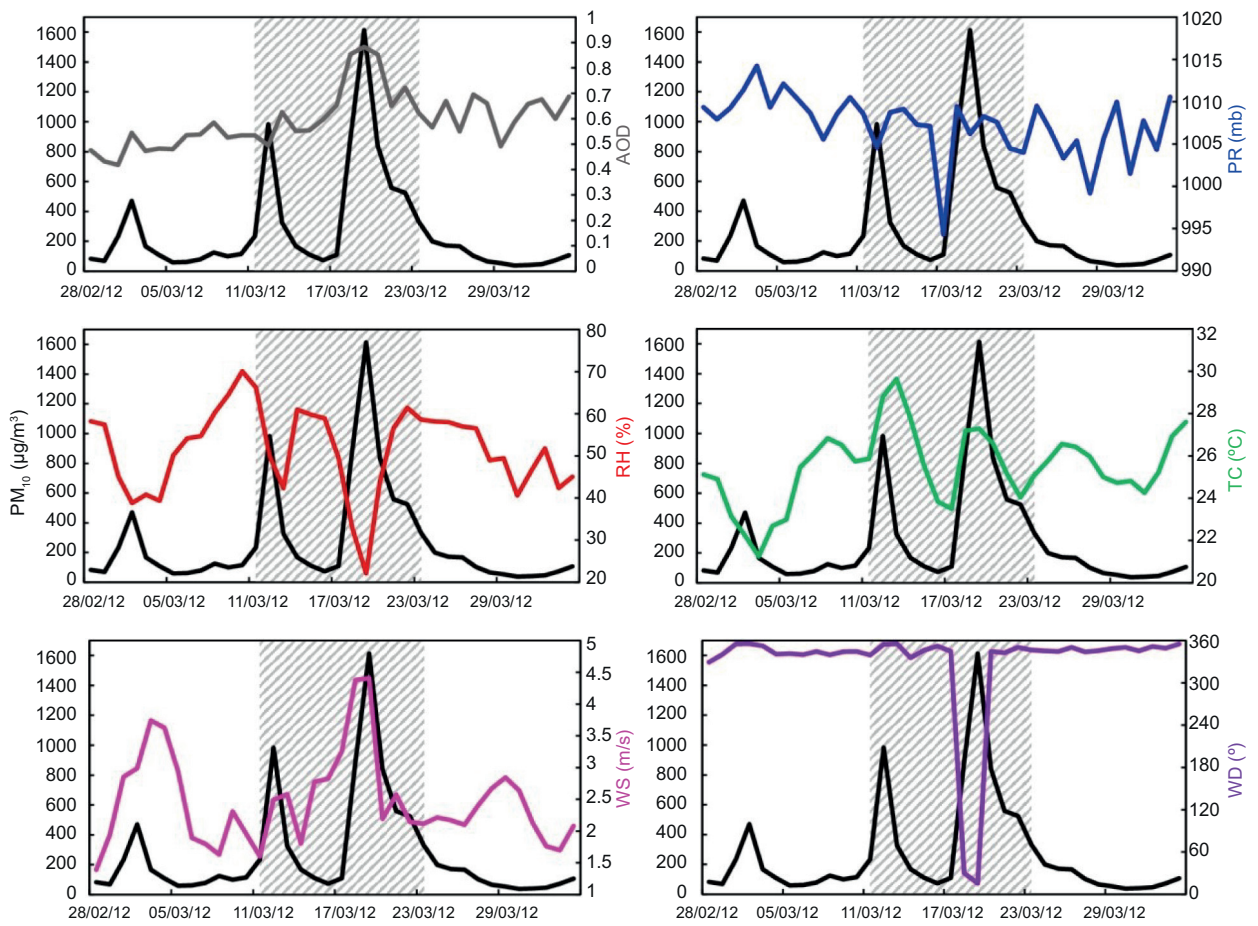
Fig. S5. Same as in Fig. S3, but for the extreme event on March 11 to 23, 2012.